FIU Institute of Environment
FLORIDA INTERNATIONAL UNIVERSITY

Monitoring of Tree Island Condition in the Southern Everglades

(Cooperative Agreement #: W912HZ-19-2-0032)

Year-4 Report (2022-2023)

Submitted to:

Ms. Sherry Whitaker
U.S. Army Engineer Research and Development Center (U.S. Army - ERDC)
3909 Halls Ferry Road, Vicksburg, MS 39081-6199
Email: Sherry.L.Whitaker@usace.army.mil

Jay Sah, Ximena Mesa, Michael Ross, Daniel Gann,
Susana Stoffella, Bianca Constant, Santiago Castaneda, Juliana Alvarez
Institute of Environment
Florida International University, Miami, FL

June 30, 2024

Authors' Affiliation

Jay P. Sah, Ph.D. – *Research Associate Professor*
Institute of Environment
Florida International University
11200 SW 8th ST, Miami, FL 33199
Tel. (305) 348-1658; Email: sahj@fiu.edu

Daniel Gann, Ph. D. – *Assistant Professor*
Department of Biological Sciences / Institute of Environment
Florida International University
11200 SW 8th ST, Miami, FL 33199
Tel. (305) 348-1971; Email: gannd@gmail.com

Michael S. Ross, Ph.D. – *Professor*
Department of Earth & Environment / Institute of Environment
Florida International University
11200 SW 8th ST, Miami, FL 33199
Tel. (305) 348-1420; Email: rossm@fiu.edu

Ximena Mesa – *Ph.D. Student/Research Assistant*
Institute of Environment
Florida International University
11200 SW 8th ST, Miami, FL 33199
Tel. (305) 348-6066; Email: xmesa@fiu.edu

Susana Stoffella – *Research Analyst*
Institute of Environment,
Florida International University
11200 SW 8th ST, Miami, FL 33199
Tel. (305) 348-0493; Email: stoffell@fiu.edu

Bianca Constant – *Field / Lab Technician*
Institute of Environment, Florida International University
11200 SW 8th ST, Miami, FL 33199
Tel. (305) 348-6066; Email: biconsta@fiu.edu

Santiago Castaneda – *Sr. Lab Technician/Lab Manager*
Institute of Environment, Florida International University
11200 SW 8th ST, Miami, FL 33199
Tel. (305) 348-6066; Email: scastane@fiu.edu

Juliana Alvarez – *Field / Lab Technician*
Institute of Environment, Florida International University
11200 SW 8th ST, Miami, FL 33199
Tel. (305) 348-6066; Email: alvarezj@fiu.edu

Cover Photo: Hardwood hammock on SS-81, a tree island located in NESRS, showing damaged sugarberry (*Celtis laevigata*) tree and recently grown young Brazilian pepper (*Schinus terebinthifolia*). Photo credit: Juliana Alvarez.

Table of Contents

General Background

Tree islands, an integral component of the Everglades, are abundant in both the marl prairie and ridge and slough landscapes. They are also likely to be sensitive to large-scale restoration actions associated with the Comprehensive Everglades Restoration Plan (CERP) authorized by the Water Resources Development Act (WRDA) of 2000 to restore the south Florida ecosystem. More specifically, changes in hydrologic regimes associated with ongoing restoration projects and operational plans, including the construction and operations of two Tamiami Bridges, implementations of Central Everglades Planning Project (CEPP) components, and Combined Operational Plan (COP) (USACE, 2014; USACE, 2020), are set to continue influencing the impact of existing local and landscape-level drivers and stressors, such as hydrology, invasive exotics, windstorms, and fire (Wetzel et al., 2017).

While the alterations in the impact of these drivers and stressors influence the spatial distribution pattern of tree islands within the landscape, the hydrologic alterations also affect the internal water economy of islands in both inland and coastal wetlands, which in turn influences plant community structure and function by affecting species composition, tree regeneration and growth (Sah et al., 2018; Ross et al., 2022; Stoffella et al., 2022). In the Greater Everglades Conceptual Ecological Model (CEM), researchers have identified plant community composition and structure of tree islands as one of several ecological attributes that are affected by changes in hydrologic characteristics, fire regimes and other stressors. When these stresses become severe, the forest's structure and function can be in peril, leading to tree island loss. For restoration purposes, it is important to project when natural and/or management-induced hydrologic conditions and other stressors will surpass the ability of islands to remain ecologically functional. Several examples of such adverse episodes have been reported. For instance, Everglades researchers showed that loss of tree islands in the Water Conservation Areas was primarily caused by management-related highwater levels due to compartmentalization of the system after 1960s (Patterson & Finck, 1999; Brandt et al., 2000). Likewise, one analysis of multi-year historical aerial photography suggested that a decline in the areal extent of tree islands also occurred within Everglades National Park (ENP) between 1952 and 2004 (Sklar et al., 2013). Though the reasons for this decline in ENP islands have not yet been fully explored, one possibility is that it reflects the effects of alterations in the Everglades' hydrologic regime either directly, or through their impact on other stressors such as fire and windstorms. Thus, for the RECOVER monitoring program, a strategy for tree island work that focuses on both local and landscape-scale effects is important.

To better understand inter-annual variability as well as long-term trends and mechanisms that drive them, it is essential to delineate patterns of community composition and configuration at high spatial precision that allow for detection of short-term fluctuations and to differentiate them from persistent long-term change. An approach that concentrates most effort on linking intensive ground surveys with extensive community patterns derived from satellite data and aerial photography and with topographic variation derived from LiDAR data is likely to help in

reaching a more nuanced understanding of past change in tree island structure, as well as in projecting responses to future changes in water level.

To strengthen our ability to assess the "performance" of tree island ecosystems and to predict how hydrologic alterations translate into ecosystem responses, an improved understanding of plant community structure and function, and their interactive responses to disturbances such as fires and hurricanes is important. Built on a baseline study of vegetation structure and composition and associated biological processes over three years (1999-2002) on three tree islands in Shark River Slough (Ross and Jones, 2004), a broader study was initiated in 2005 and has been continued through today. While the initial (1992-2003) tree island work was supported by the National Park Service (NPS) through the Department of Interior's Critical Ecosystems Study Initiative (CESI), for four years (2005-2009) the project was funded alternatively by the US Army Corps of Engineers (USACE) and South Florida Water Management District (SFWMD), directly or indirectly through ENP. Since 2009, the study has been funded by the US Army Corps of Engineers (USACE) through its contracting office US Army Engineers Research and Development Center (ERDC). Until the Fall of 2014, the study was led by Dr. Michael Ross. Thereafter, the study has been led by Dr. Jay Sah, while Dr. Michael Ross and Dr. Daniel Gann are actively involved as the Co-PIs in the study. The comprehensive results of work accomplished through 2014 are described in Ruiz et al., (2011, 2013) and Sah et al., (2012, 2015). The results of the thorough analysis of vegetation dynamics over 20 years (1999-2019) and detailed results of work accomplished between 2014 and 2019 are described in Sah et al., (2020). A new phase of the project was initiated in Fall 2019 (Cooperative Agreement # W912HZ-19-2-0032). The results of the study completed during the first year (2019-2020), second year (2020-2021) and third year (2021-2022) of this phase are described in three annual reports (Sah et al., 2021, 2022 and 2023), respectively.

The major goal of ongoing monitoring of southern tree islands is to assess structural and compositional responses of tree island vegetation to natural and management-induced hydrologic change, alterations in relative proportion of forest communities on the islands, and the expansion or contraction of islands within their surrounding marshes. This research addresses the relevant RECOVER performance measures (PM), (1) GE-15: 'Ridge and Slough Sustainability', and (2) 'Total System Performance Measure (RECOVER, 2011). The working hypothesis of the study is expressed as 'the loss of elongated patterns of ridges, sloughs, and tree islands in the direction of water flow in the ridge and slough landscape of the Everglades is attributed to disrupted sheet flow and related changes in water depth' identified in the hypothesis cluster of the sub-section 3.3.7.1 of the 2009 CERP Monitoring and Assessment Plan (RECOVER, 2009). The ongoing work is also linked to the most recent update of Greater Everglades Landscape hypothesis cluster, namely "Interrelationships of Sheet Flow, Water Depth Patterns, Oligotrophic Nutrient Status, and Landscape Patterns" (*in progress*).

Since 2012, the study has linked field sampling (in a network of permanent plots and along transects) and remote sensing activities to establish a more complete, spatially explicit

inventory of vegetation patterns within individual tree islands, one that can be used to monitor vegetation change in a consistent and repeatable way.

The specific objectives of our ongoing research are:

1. To assess temporal changes in the structure and composition of both swamp forest and hardwood hammock.

2. To determine the relationships among the hydrologic regimes of adjacent marshes, other stress variables, and dynamics of vegetation communities on tree islands.

3. To develop a tree island plant community/vegetation classification based on canopy and understory vegetation types along the full elevation gradient from hardwood hammock to surrounding marshes for each tree island.

4. To develop and validate classification algorithms based on bi-seasonal spectral reflectance models and LiDAR derived canopy height models that allow for consistent and repeatable delineation of vegetation assemblages and to delineate their boundaries and changes of boundaries.

5. To scale the vegetation classes to remote sensor resolutions that are available for the past 35+ years and to map the communities at multiple spatial resolutions and multiple thematic class details.

6. To detect and map changes and trends in aerial extent of the relative proportion of different vegetation communities from the long-term remotely sensed record from the lower resolution spectral data.

7. To investigate the correlation of spatially explicit long-term vegetation changes in response to hydrological regime changes.

This document describes the results of the work accomplished in Year-4 (Option Year 3: 2022-2023) of the five-year (2019-2024) project (Cooperative Agreement # W912HZ-19-2-0032). In WY 2021/22, four bayhead swamp plots, one each in Chekika, Irongrape, NP-202 and Vulture islands, were established and sampled for the first time. However, this report does not include the analysis of that data, which will be included along with data from the Bayhead and Bayhead swamp plots on our other four islands, in Option Year-4. This year's report is organized in two sections. Section 1 focuses on tree layer and understory vegetation dynamics in hardwood hammock portions of eight tree islands in ENP. Note that detailed vegetation study in the hardwood hammock plots was done on only four islands in 2020-21, 2021-22 and 2022-2023. The primary focus of this section of this year report is on vegetation responses to annual hydrologic changes and recovery after Hurricane Irma. Section 2 summarizes plant community distributions determined by fine-scale vegetation mapping on eleven tree islands, five located in the Shark River Slough (SRS), five in Northeast Shark River Slough (NESRS) and one in prairie along the eastern boarder of the Everglades National Park (ENP).

1. Effects of hydrology and hurricane on vegetation dynamics in tree island hardwood hammocks of the southern Everglades

1.1 Introduction

Tree islands are a prominent feature in both the marl prairies (MP) and ridge and slough (R&S) landscapes of the Everglades. In the R&S landscape, flow-induced teardrop-shaped tree islands often include different plant communities - tropical hardwood hammock, bayhead forest (hereafter called 'bayhead') and bayhead swamp - arranged along topographic, hydrologic and soil nutrient gradients (Armentano et al., 2002; Sah, 2004; Espinar et al., 2011; Sah et al., 2018). Despite the small areas they cover, the hardwood hammock-dominated heads are of great ecological significance, as both biodiversity and phosphorus 'hotspots' within the homogeneous oligotrophic landscape (Ross and Jones, 2004; Wetzel et al., 2008). While hydrology plays an important role in the development and maintenance of the ridge-slough-tree island patterned landscape, the associated plant communities also influence the hydrodynamics and spatial distribution of soil resources, which in turn affect ecological processes on tree islands (Ross and Jones, 2004; Ross et al., 2006; Givnish et al., 2008; Hanan and Ross, 2010; Espinar et al., 2011; Ross and Sah, 2011; Sullivan et al., 2010, 2013; Wetzel et al., 2005, 2017; Sah et al., 2018) (Figure 1.1).

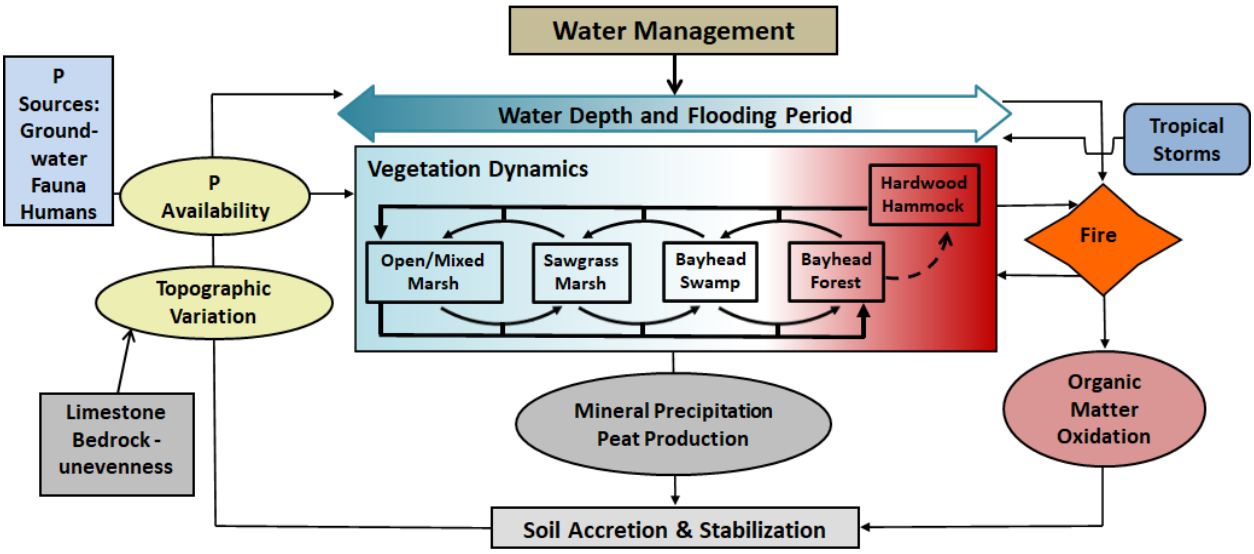

Figure 1.1 A conceptual model: vegetation dynamics in tree islands and surrounding marsh.

Beyond the physiographic template, the species assemblages and areal extent of different plant communities on the R&S tree islands, and between tree islands and adjacent marsh fluctuate significantly over time depending on the climate and anthropogenically induced changes in flooding and fire regimes (Stone and Chmura, 2004; Bernhardt and Willard, 2009). In R&S tree islands, the swamp forests and tails are usually the areas that respond most noticeably to hydrologic changes. In recent years, increase in water delivery into ENP under the Increment

Field Tests associated with the Combined Operation Plan (COP) and then implementation of the Plan, has resulted in increased water level in NESRS (Sarker et al., 2020), which has caused marsh vegetation to shift towards wetter type (Nocentini et al., 2024). After the full implementation of COP in August 2020, water delivery into ENP, especially to NESRS, has increased. For instance, in WY2021 and 2022, the volume of water delivered to NESRS across Tamiami Trail was 71.0% and 84.6% higher than the volume delivered in WY2020 (USACE, ENP and SFWMD, 2023). Vegetation community on a tree island (SS-81) in that region has already been showing impact of an increase in water level in the area (Sah et al., 2023). Since the volume of delivery to the NESRS region is projected to increase further in coming years, it is likely to continue affecting vegetation composition on the tree islands in that region.

In the hardwood hammocks, which are rarely flooded and often have a mean annual water table below 40 cm, tree species composition is also the legacy of long-term interaction between water levels and other physical processes, including recurrent tropical storms (Ruiz et al., 2011; 2013, Sah et al., 2018). In these islands, plant communities recover within a few years after a hurricane. However, vegetation recovery also depends on the post-hurricane environmental conditions. On September 10, 2017, Hurricane Irma made landfall in the Florida Keys as a Category 4 hurricane, and then struck the southwest coast of Florida as a Category 3 hurricane (Cangialosi et al., 2018). However, its impact was felt in most of south Florida. A preliminary analysis of 2017 (WY 2017/18) and 2018 (WY 2018/19) tree data revealed severe damage to trees in eight tree islands for which pre-Irma data were available. Post-Irma assessment of tree damage in these hardwood hammocks served as baseline data to follow the vegetation recovery from the damage. An assessment of recovery from hurricane damage for the five post-Irma years has shown a difference in responses among species on the monitored islands (Sah et al., 2023). A continued assessment of vegetation dynamics on these islands is expected reveal the islands' resilience, i.e., their capacity to recover since the last disturbance.

This section of the report includes the results of the continued monitoring of tree layer vegetation structure and composition in hardwood hammocks on a subset of four tree islands within a 16-island network established in ENP for long-term monitoring and assessment (Shamblin et al., 2008; Ruiz et al., 2011). It also includes the post-Irma assessment of vegetation on those four islands and an additional four tree islands for which pre-Irma vegetation composition data were available.

1.2 Methods

1.2.1 Study Area

The eight tree islands which have recently been monitored represent a subset of those 16 islands that were intensively studied between 2005 and 2010. These islands included one prairie island (Grossman Hammock) along the eastern border of the ENP, four islands (Black Hammock, Gumbo Limbo, Satinleaf, and Vulture Hammock) in Shark River Slough (SRS), and three (Chekika, Irongrape and SS-81) in Northeast Shark River Slough (NESRS) (Figure 1.2).

Two islands, SS-81 and Chekika are located immediately downstream from the 1-mile (eastern) and 2.6-mile (western) bridges on Tamiami Trail, respectively, and they are likely to exhibit the impacts of increased flow from the WCAs into ENP as time goes on.

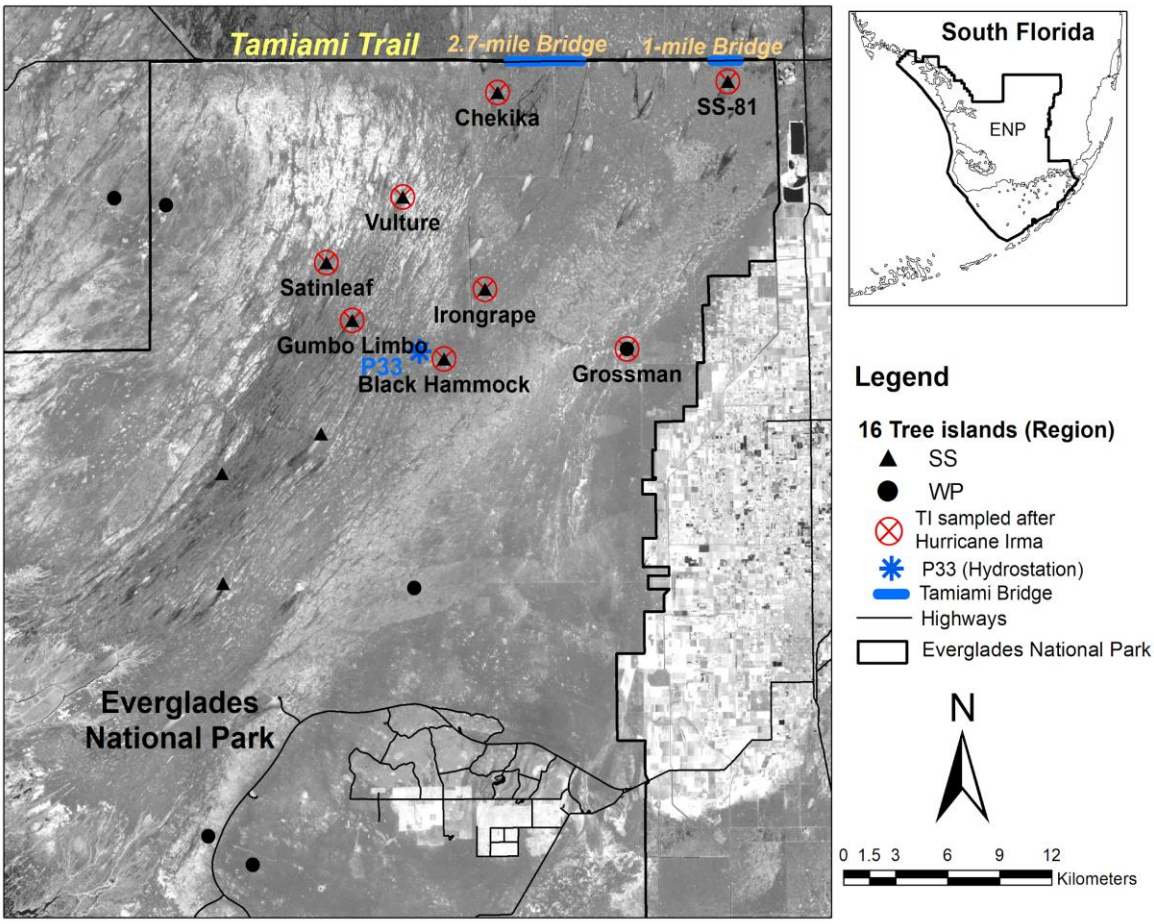

Figure 1.2 Location map of tree islands that have permanent plots in hardwood hammocks. The plots have been sampled during various periods between WY 2000/01 and 2022/23. In the first three years (WY 2017/18, 2018/19, 2019/20) after hurricane Irma, vegetation was re-sampled on eight tree islands, and in the next three years (WY 2020/21, 2021/22 and 2022/23) sampling was done on only four islands.

1.2.2 Data Collection

1.2.2.1 Vegetation sampling

The vegetation sampling in the hardwood hammock plots was organized in a nested design that accounted for all the major forest strata (trees & saplings, shrubs, seedlings, and herbaceous macrophytes). The sampling protocol followed the methodology described by Sah (2004) and Ruiz et al., (2011). Between WY 2011/12 and 2016/17, tree layer vegetation was sampled in the hardwood hammock plots on four islands: Black Hammock (BL), Gumbo Limbo (GL), Satinleaf (SL) and SS-81 (Heartleaf: HL). However, following Hurricane Irma, both tree and herb layer vegetation were sampled for the six years (WY 2017/18 to 2022/23) on those four

islands, and for three years (WY 2017/18 to 2019/20), on another four islands (Chekika Island (CH), Grossman Hammock (GR), Irongrape (IG), and Vulture Hammock (VH)). The size of monitoring plots on these eight islands ranged between 300 m^2 in SS-81 to 625 m^2 in Gumbo Limbo and Satinleaf (Table 1.1).

Table 1.1 Location and topographic data (mean, minimum, and maximum) of hardwood hammock plots on eight tree islands.

Tree Island	Easting NAD83 (UTM_Z17N)	Northing NAD83 (UTM_Z17N)	Plot Size (m^2)	Mean (± 1 S.D.) Plot Elevation (m NAVD 88)	Minimum Plot Elevation (m NAVD 88)	Maximum Plot Elevation (m NAVD 88)	Island height (cm)**
Black Hammock	531295	2832630	400	2.330 ± 0.166	1.988	2.584	99.1
Chekika	534372	2847485	400	2.624 ± 0.035	2.545	2.712	113.8
Grossman	541819	2833205	400	2.042 ± 0.144	1.386	2.238	44.5
Gumbo Limbo	525999	2834793	625	2.059 ± 0.071	1.916	2.24	87.8
Irongrape	533651	2836523	400	2.240 ± 0.050	2.092	2.345	92.0
Satinleaf	524499	2838019	625	2.221 ± 0.076	2.082	2.368	89.3
Heartleaf (SS-81)	547639	2848113	300	2.168 ± 0.304	1.592	2.649	80.0
Vulture	528918	2841667	400	2.663 ± 0.191	2.338	2.977	127.7

Each plot is gridded into 5×5m cells, whose corners and midpoint are marked by 30 cm long flags and ½″ PVC stakes affixed to the ground, respectively. When the plots were first established on these islands, the plot and cells were set up using compass, measuring tape, sighting pole(s), and right-angle prism. In these plots, all trees (≥5 cm) are tagged with numbered aluminum tags, and the location of each tagged tree is recorded to the nearest 0.1m using the SW corner of the plot as a reference (0, 0). Furthermore, if a tree has multiple stems ≥5 cm diameter (cm) at breast height (DBH), each stem is tagged with a unique ID that allows it to be cross-referenced back to its 'parent' stem. Status (live and dead) and DBH of each individual tree was first recorded when plots were established (in Black Hammock, Gumbo Limbo and Satinleaf in 2001, and in SS-81, Chekika, Grossman, Irongrape and Vulture Hammock in 2007).

Within each plot, the status (live and dead) of tagged trees and the presence of any tree that had grown into the >5cm DBH class (hereafter called ‘ingrowth’) since the previous survey were recorded. Ingrowths were identified to species, tagged, and their DBH was measured. The density and species of all tree saplings (stems 1-5 cm in DBH) within each 5 x 5 m cell were also recorded, and the samplings were assigned to one of two DBH size classes: 1-3 cm or 3-5 cm. The density of woody seedlings (stems < 1 m) and shrubs (stems > 1 m and < 1 cm DBH) was estimated in nested circular plots of 1.0 m^2 and 3.14 m^2, respectively, centered on the midpoint of each cell. Seedlings present within the 1 m^2 (0.57 m radius) plots were counted and identified to species and assigned to one of three height categories (1-30, 30-60, and 60-100 cm). Shrubs rooted within the 3.14 m^2 (1 m radius) plots were counted and identified to species. The total cover of each shrub species was also estimated using a modified Braun-Blanquet scale based on the following six cover categories: Cat 1: <1%; 2: 1-4%; 3: 4-16%; 4: 16-32%; 5: 32-66%; & 6:

>66% (Sah, 2004). Within the 1 m radius plot, the total cover of all herbaceous macrophytes, which includes seedlings, shrubs (< 1 m tall), epiphytes, vines, and lianas, was also estimated by species, using the same cover scale.

Canopy closure was estimated by taking two densiometer readings, one facing north and one facing south, at the midpoint of each cell (Lemmon, 1956). The densiometer estimates of forest canopy closure were supplemented with hemispherical canopy photographs. At the midpoint of each cell, a hemispherical photo of the canopy directly overhead was taken using a Nikon 950 digital camera with a Nikon FC-E8 fisheye lens adapter (NIKON Inc., Melville, NY), placed and leveled 1.5 m above the ground. Leaf area index (LAI) was calculated by processing the hemispherical canopy photos with the Gap Light Analyzer program, GLA 2.0 (Frazer et al., 1999). For each hemispherical image, we calculated the percent canopy openness and the 4-ring LAI – the ratio of the total one-sided leaf area to the projected ground area (Parker, 1995).

1.2.2.2 Hydrology

For hardwood hammock plots in each of the study islands, ground elevation data were available from detailed topographic survey conducted using auto-level from either a 1st order vertical control monument (benchmark) or from a reference benchmark established in the marsh, followed by an estimate of benchmark elevation by differential GPS; in some cases, benchmark elevation was calculated by relating water depth at the benchmark to the estimate of water surface elevation at that location and time from EDEN (Everglades Depth Estimation Network) (Ruiz et al., 2011). In conjunction with the daily EDEN water surface elevation data (http://sofia.usgs.gov/eden), elevation of the ground surface within the plots was then calculated.

1.2.3 Data Analysis

1.2.3.1 Hydrologic conditions

Mean annual and seasonal water depths (hereafter called relative water level (RWL)), and discontinuous hydroperiod (the number of days in a year when water is above the ground surface) were estimated based on ground elevation and the time series data of water surface elevation (WSE) extracted from EDEN database. Previous studies have found that prairie and marsh vegetation composition are well predicted by the previous 3-5 years of hydrologic conditions (Armentano et al., 2006; Zweig and Kitchens, 2009), whereas tree island vegetation was found strongly correlated with 7-year average hydroperiod and water depth (Espinar et al., 2011; Sah, 2004; Sah et al., 2018). Thus, in this study, we averaged hydroperiod and mean annual RWL for 7 water years (May 1st – April 30th) prior to each sampling event to examine the relationships between hydrologic parameters and change in vegetation characteristics. In addition, we also calculated long-term (32 years; WY 1991/92-2022/23, the period for which EDEN data are available) average of mean annual water level to examine the annual deviation of RWL from the long-term average.

1.2.3.2 Tree-layer vegetation dynamics

Tree census data were summarized by calculating annual mean tree mortality and ingrowth, two important indicators of woody vegetation dynamics. In addition, tree density and basal area for each species were calculated and summed to produce totals for each island.

Differential mortality and/or ingrowth among species over time can result in changes in species composition. These changes were analyzed using non-metric multidimensional scaling (NMDS) ordination. Species abundance data used in the ordination was the species importance value (IV). Tree density and basal area for each species were summed for each plot, relativized as a proportion of the plot total, and used to calculate Importance Value (IV) of species using the following equation: $IV = 100 \bullet ((R_{den} + R_{ba}) / 2)$, where R_{den} is the species relative density and R_{ba} is the species relative basal area. Importance value (IV) data of each species were standardized to species maxima and the Bray-Curtis (B-C) dissimilarity index was used as a measure of dissimilarity in the ordination. Relationships between species composition and environmental vectors representing topography and hydro-edaphic characteristics (relative water level, TI_Ht, soil depth, soil phosphorus and total organic carbon) were examined.

1.2.3.3 Herb/Shrub layer vegetation dynamics

We characterized changes in shrub and herb species composition and examined vegetation:environment relationships using NMDS ordination. Species abundance data used in the ordination was species' mean percentage cover, however species present in only one plot were discarded. The cover values for each species were relativized to plot total cover and the Bray-Curtis (B-C) dissimilarity index was used as a measure of dissimilarity in the ordination. Relationships between species composition and environmental vectors representing, topographic, hydro-edaphic characteristics (relative water depth, TI_Ht and soil depth) and tree canopy cover were examined using a vector-fitting procedure incorporated in the computer R package VEGAN (Oksanen et al., 2022; R Core Team 2024). Ordination axes were rotated so that Axis 1 was aligned with the relative water depth (RWL).

1.3 Results

1.3.1 Hydrologic conditions

Hydrologic condition in tree island hammocks varies depending on the location of tree islands within the R&S landscape and tree island height above the surrounding marshes. On the eight tree islands, the annual mean (±SD) relative water level (RWL) over seventeen years (WY 2006/07 to 2022/23) ranged between -92.0 ± 14.0 cm in Chekika and -55.2 ± 17.4 cm in SS-81 (Table 1.2). The mean RWL in each Chekika, Vulture, and Black Hammock was 19.8-28.8 cm lower than that in other tree islands individually, suggesting that island height, i.e., the difference between average plot elevation and adjacent marsh ground elevation, of these three islands are higher than other islands. Also, within the hammock plot on each island, annual mean RWL was not uniform. Average within plot variation (Coefficient of variation, CV) in annual mean water level was the highest in SS-81 (CV = 44.6%), and the lowest in Chekika (CV = 2.9%).

Table 1.2 Annual mean (±SD) relative water level (RWL) averaged over 17 years (WY 2006/07 to 2022/23) in the hardwood hammock plots on eight tree islands.

Tree Island	Relative water level (RWL) (cm)		
	Annual Mean (± S.D.)	Annual Range (Min-Max)	Within plot variation (CV %)
Black Hammock	-84.0 ± 10.0	-100.5 to -66.4	-17.5
Chekika	-90.2 ± 14.0	-114.2 to -63.5	-2.9
Grossman	-63.8 ± 17.5	-91.5 to -32.4	-15.2
Gumbo Limbo	-58.0 ± 9.8	-74.0 to -41.8	-11.2
Irongrape	-64.2 ± 10.9	-81.7 to -43.8	-6.4
Satinleaf	-64.2 ± 9.8	-79.0 to -48.2	-11.4
Heartleaf (SS-81)	-55.2 ± 17.4	-84.2 to -22.6	-44.6
Vulture	-90.2 ± 10.8	-108.0 to -72.9	-19.2

Over the last seventeen years, the RWL varied annually. Between WY 2006/07 and WY 2011/12, the annual mean RWL was 1.4 to 28.2 cm lower than the 32-year (WY 1992-2023) average (Figure 1.3). In contrast, the RWL in the most recent 11-year period (from WY 2012/13 to 2022/23) was 0.1 to 33.5 cm above the 32-year average, except in WY 2014/15, 2015/16 and 2019/20, when mean RWL in most of the islands was 0.9 to 14.1 cm below the long-term average. However, in 2015/16, two islands (Grossman, and Gumbo Limbo) and in 2019/20, two islands (Chekika and SS-81) had mean RWL higher than 32-year average. Likewise, in WY 2012/13 and 2018/19, when majority of islands had high water levels, one island (Chekika) in WY 2012/13 and three islands (Gumbo Limbo, Satinleaf and Vulture) had lower RWL than 32-year average.

Among all these seventeen years, 2022/23 was the wettest year when the annual mean RWL was 14.2 cm (in Satinleaf) to 33.5 cm (in SS-81) higher than the long-term average. Since WY 2006/07, for most years none of the hammock plots on these eight islands, except SS-81,

were inundated. However, in WY 2017/18 and 2020/21, the high-water level on many of these islands was observed. In 2017/18, characterized by the extremely high-water levels in Hurricane Irma's aftermath, plots on 7 of 8 islands, except Chekika, were partly inundated for varying periods. One sub-plot in Black Hammock and seven sub-plots on Irongrape was inundated for only one or two days, whereas a sub-plot in SS-81 was inundated up to 184 days. In fact, seven sub-plots on Gumbo Limbo and six on Satinleaf were inundated for 7-90 days in the same water year. Moreover, the aforementioned sub-plot in SS-81 in NESRS was inundated for 1 to 331 days in 14 of 17 years between WY 2006/07 and 2022/23, and for more than 100 days since 2015/16, when water delivery under Increment Field Tests began in October 2015 (USACE, 2020), and water level on this island has significantly ($r = 0.97$, $p < 0.001$) increased. On this island, a second subplot was inundated for 37-237 days during the last six (WY 2017/18-2022/23) water years. Actually, 40% of the hardwood hammock plot on SS-81 was inundated for various period during the last three (2020/21 - 2022/23) water years, and the inundation period in the hardwood hammock plot on this island is likely to continue increasing with an increase in water delivery into ENP.

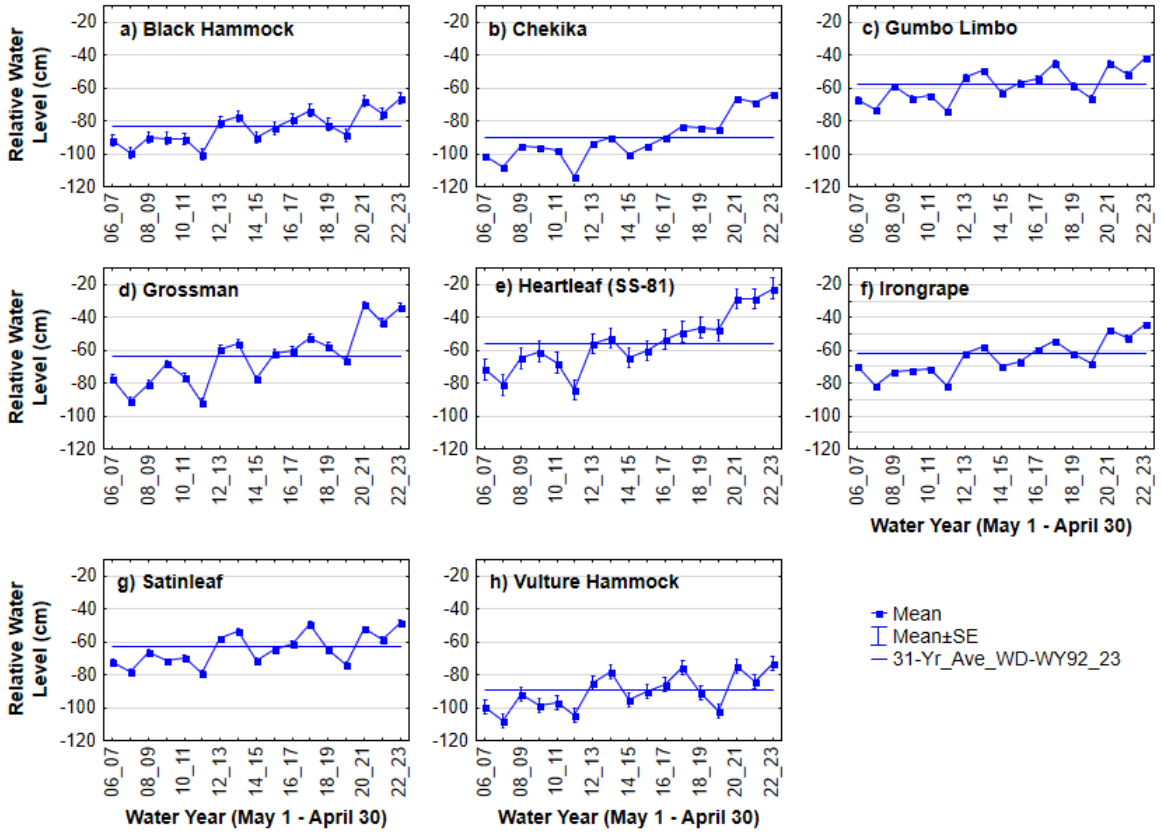

Figure 1.3 Annual mean (±SE) relative water level (RWL) for the period of Water Year 2006/07 – 2022/23 and long-term (WY 1991/92-2022/23) average RWL in the hardwood hammock plots on eight tree islands. For each hammock plot, RWL was averaged over 12 to 25 5x5m sub-plots. RWL for sub-plot was calculated by subtracting mean elevation of subplot from EDEN water surface elevation (WSE) at the hammock plot.

In general, the annual mean water level in these hammocks followed the regular dry (low) and wet season (high) pattern. However, in some years, water level in the hammock plots was much higher in the dry season than the wet season due to either an anomaly in weather pattern, management-induced changes in hydrologic regime, or both. For instance, over the last 16 years, the most remarkable discrepancy between dry and wet season pattern was in 2011/12, 2015/16, 2020/21 and 2021/22, when the water level was higher, i.e., much closer to the ground surface (<40 cm; in SS-81 <20 cm), in the dry season than in the wet season (Figure 1.4). Likewise, annual mean dry and wet season water levels were almost the same in 2009/10, 2014/15 and 2017/18. This was caused by unusually high dry season (winter) rainfall followed by the very dry wet season as well as the increased water deliveries into ENP in the dry season. In those years, the discrepancies in dry and wet season water level were more distinct in NESRS and Prairie islands (Figure 1.4 b, d, e) than in SRS islands.

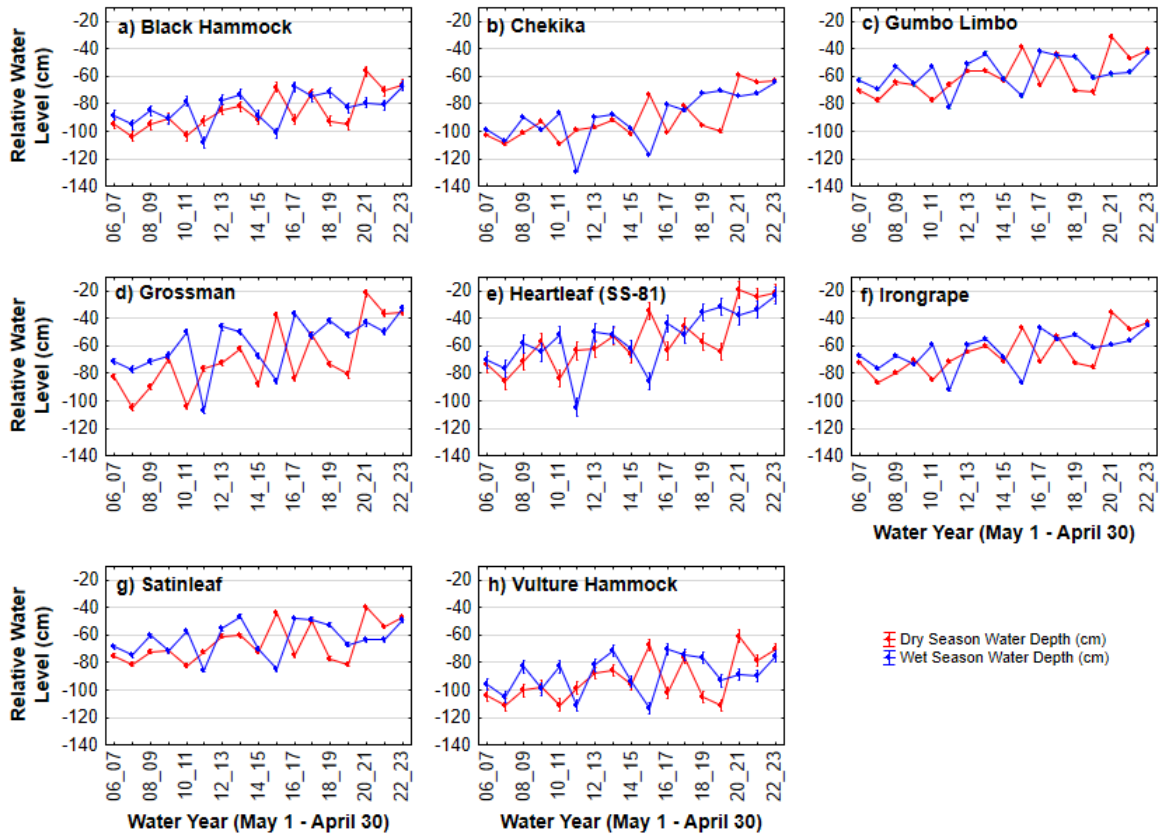

Figure 1.4 Seasonal mean (±SE) relative water level (RWL) in the hardwood hammock plots on eight tree islands. For each hammock plot, RWL was averaged over 12 to 25 5x5m sub-plots. RWL for sub-plot was calculated by subtracting mean elevation of subplot from EDEN water surface elevation (WSW) at the hammock plot.

In South Florida, including the Everglades, winter rainfall is strongly linked to El Niño events. In the WY 2015/16, WY 2020/21 and WY 2022/23 dry season rainfall was higher than historical average of season rainfall (Abtew and Ciuca, 2017; Cortez et al., 2022; Cortez, 2024), resulting in high water conditions throughout South Florida, especially the Water Conservation Areas (WCAs). That prompted emergency operations to move water to the south, i.e., into Everglades National Park (ENP). These unusual emergency deviation during the dry seasons and

increased water delivery into ENP resulting from both MWD Increment Field tests followed by the full implementation of Combined Operational Plan (COP) in August 2020 (USACE, ENP and SFWMD, 2023) have contributed to the spatial and temporal differences in water conditions within the Everglades tree island hammocks. In fact, mean annual RWL in these islands in SRS and NESRS is hardly in tandem with the total annual rainfall in that region. For this analysis, stage recorder P33 located in SRS (Figure 1.2), for which long-term rain data are available on DBHYDRO (www.sfwmd.gov/science-data/dbhydro), was used. Between 2006/07 and 2022/23, a correlation between annual total rainfall at P33 and mean RWL on each of these eight islands was not significant (Figure 1.5; p-value>0.05), because the hydrologic conditions in these islands depend in large part on the water delivery from the adjacent WCA 3A and 3B.

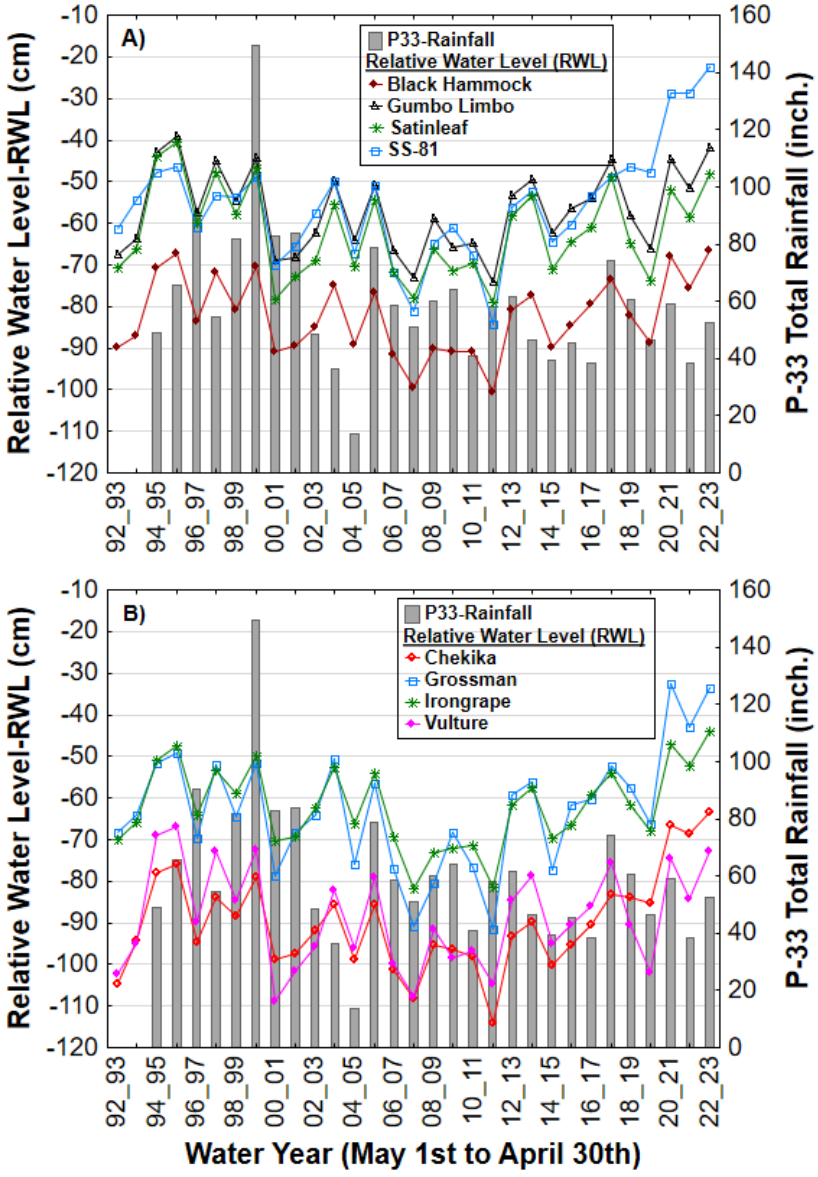

Figure 1.5 Relationship between annual total rainfall at P33 stage recorder and mean annual relative water level (RWL) in two groups of tree islands: (A) four tree islands sampled annually, and (B) four tree islands first sampled between 2006/07 and 2010/11, and then again three times between 2017/18 and 2022/23.

1.3.2 Tree mortality and ingrowth

On tree islands, tree layer vegetation dynamics are a function of tree mortality and ingrowth, two important indicators of woody vegetation dynamics in forest ecosystems. Over four years, (WY 2007/08 to 2010/11), when the hardwood hammock on all 16 islands were studied, mean annual tree mortality on those islands was 3.6%, and both NESRS and SRS islands had higher mortality than MP islands (Figure 1.6). During those years, mean tree ingrowth was significantly higher (paired t-test, $P < 0.001$) than mean tree mortality. On average, the mean tree ingrowth was 110 trees ha^{-1} $year^{-1}$ whereas tree mortality was 53 trees ha^{-1} $year^{-1}$. Ingrowth on some islands was higher also because of recovery from Hurricane Wilma in 2005.

Between WY 2011/12 and 2016/17, hardwood hammocks of only four islands (Black Hammock, Gumbo Limbo, Satinleaf, and SS-81) were studied, and on those islands, both the mean tree ingrowth and mortality showed slight variation, except on three SRS islands in 2014. In general, annual mean mortality was slightly higher than mean ingrowth. On these four islands, the mean mortality rate was significantly different between both periods, before 2011/12 (3.62%) and between 2011/12 and 2016/17 (the years when islands were sampled before Hurricane Irma) (3.13%), whereas the mean ingrowth dropped from 6.96% $year^{-1}$ to 2.78% $year^{-1}$.

After 2016/17, both tree ingrowth and mortality on the studied tree islands varied greatly. On some islands, tree mortality drastically increased in 2017/18, mostly caused by Hurricane Irma. After the hurricane in WY 2017/18, we sampled vegetation on four additional tree islands (Chekika, Grossman, Irongrape and Vulture), all from the same network of 16 islands within ENP (Ruiz et al., 2011). Post-hurricane survey on these four islands continued for three years. In the first post-Irma year, the NESRS tree islands, especially Irongrape (NAD83 UTM Zone-17: 533651, 2836523) had exceptionally high (> 200%) ingrowth, mostly due to regeneration of papaya (*Carica papaya*) - an ephemeral semi-woody pioneer that recruits profusely from the seedbank but would disappear from the canopy within a couple of years (Sah et al., 2020).

Of the eight tree islands, tree mortality on four islands was higher in 2017/18 than in previous years (Figure 1.7). In 2017/18, i.e., within 2-4 months after Hurricane Irma, increased tree mortality was observed in Black Hammock, Grossman, Satinleaf and SS-81. Among these four islands, Black Hammock and Satinleaf were severely impacted by hurricane (Sah et al., 2020). One year after the hurricane, i.e., in 2018/19, exceptionally high mortality (>25%) was observed on Irongrape, primarily because not only many *Carica papaya* individuals that had appeared during 2017/18 died that year, even one fourth of the hardwood trees died in that year. In the following year, i.e., in 2019/20, two years after Hurricane Irma, while mortality was relatively high on 7 of 8 islands, an increase in mortality in comparison to previous year was observed only on 4 islands (Grossman, Gumbo Limbo, SS-81, and Vulture). In the following years, i.e., in 2020/21, 2021/22 and 2022/23, only four annually monitored islands were studied. During those years, high mortality was observed on two islands, Black Hammock, and SS-81. The elevated rate of mortality observed on Black Hammock after three years of the hurricane could be due to delayed mortality after the hurricane. However, on tSS-81, located downstream

of the 1-mile Tamiami Bridge and impacted by hydrologic changes in NESRS region, tree mortality rates in 2020/21, 2021/22 and 2022/23 were still high, but lower than in 2019/20 (Figures 1.7).

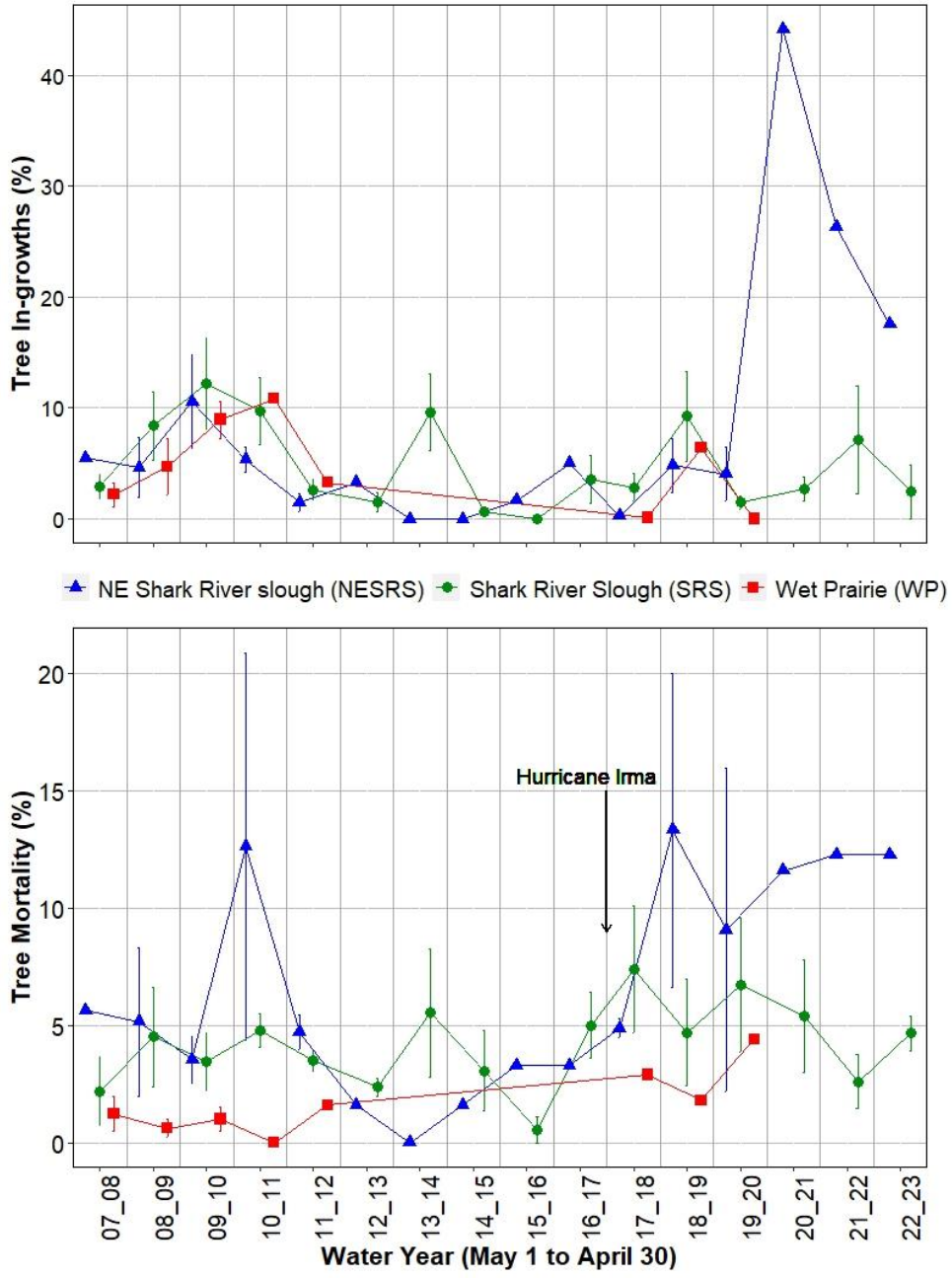

Figure 1.6 Annual mean (±) tree ingrowth (A) and mortality (B) on the tree islands monitored in Shark River Slough (SRS), Northeast Shark River Slough (NESRS) and Wet Prairies (WP) within the Everglades National Park between WY 2007/08 and 2022/23. The number of tree islands studied varied among years. Between 2012/13 and 2016/17, and in 2020/21 and 2022/23, hardwood hammocks were studied on only four islands (Black Hammock, Gumbo Limbo, Satinleaf and SS-81).

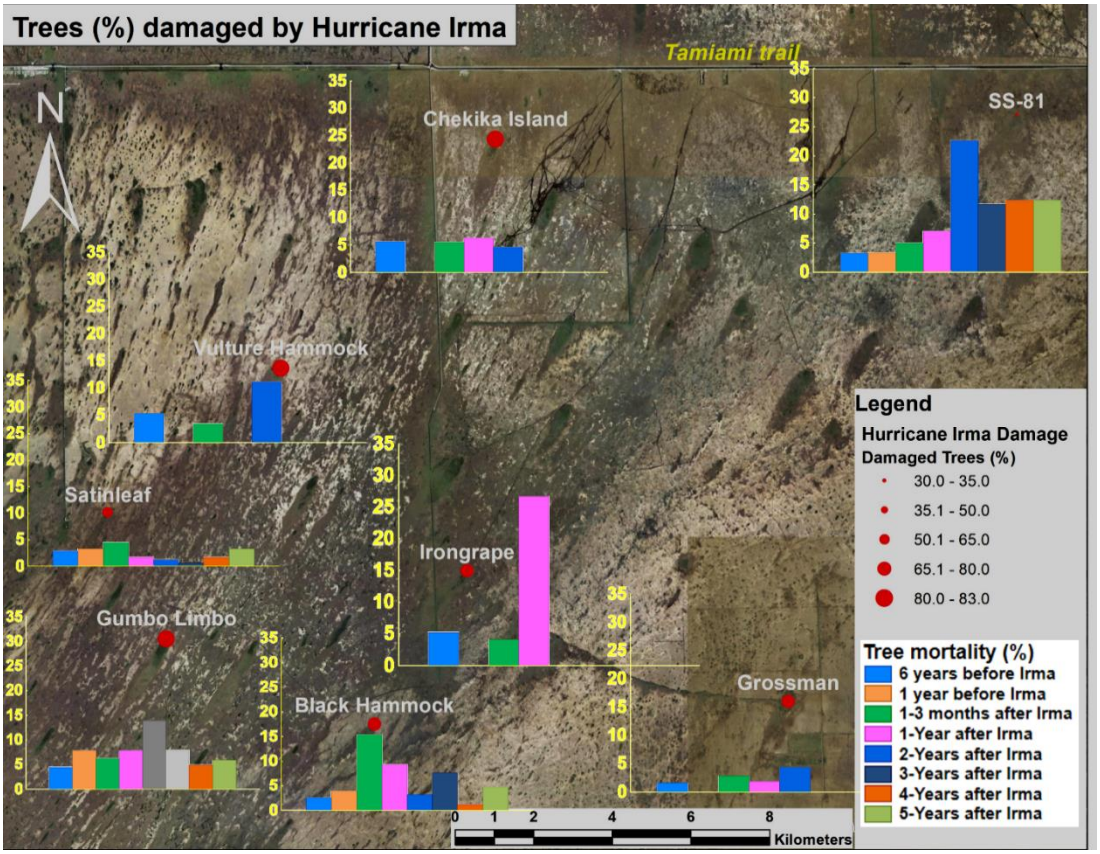

Figure 1.7 Post-Irma tree damage and annual mean tree mortality (%) on eight tree islands before and up to five years after hurricane Irma. On four islands (Chekika, Grossman, Irongrape and Vulture), pre-Irma tree mortality data were available for only 2010/11 or 2011/12, and those islands were sampled only for three years after hurricane Irma.

On the SS-81, when the hardwood hammock was studied for the first time in 2007/08, sugarberry (*Celtis laevigata*) has been a dominant species, constituting 82.7% of all trees present within the plot. Even in WY 2019/2020, the proportion of Sugarberry trees was 72.2%. However, two years later, in 2021/22, the proportion of sugarberry was only 24.2% of all trees, and that proportion dropped to 17.3% in 2022/23, indicating high mortality of this species or ingrowths of other species. In fact, in WY 2020/21, 2021/22 and 2022/23, the mortality rate of Sugarberry was 16.6%, 20.7% and 33.3%, respectively, while total ingrowths of all species were 633 trees (44.2%), 500 trees (26.3%) and 333 trees (17.5%) ha^{-1} $year^{-1}$, respectively (Figure 1.8d). It is remarkable to note that ingrowths in those three years were mostly of the exotic species, Brazilian pepper (*Schinus terebinthifolia*). A significant ingrowth of Brazilian pepper trees (>40% of all ingrowths) was also observed on Gumbo Limbo in both 2021/22 and 2022/23.

As reflected by variation in annual mean tree mortality and ingrowth, the short-term trend of tree dynamics observed in the hardwood hammocks on four islands, which were studied annually, is in accord with variation in hydrologic condition, and both the tree mortality and ingrowth were significantly affected by mean annual RWL annual variation in hydrologic conditions (Figure 1.9).

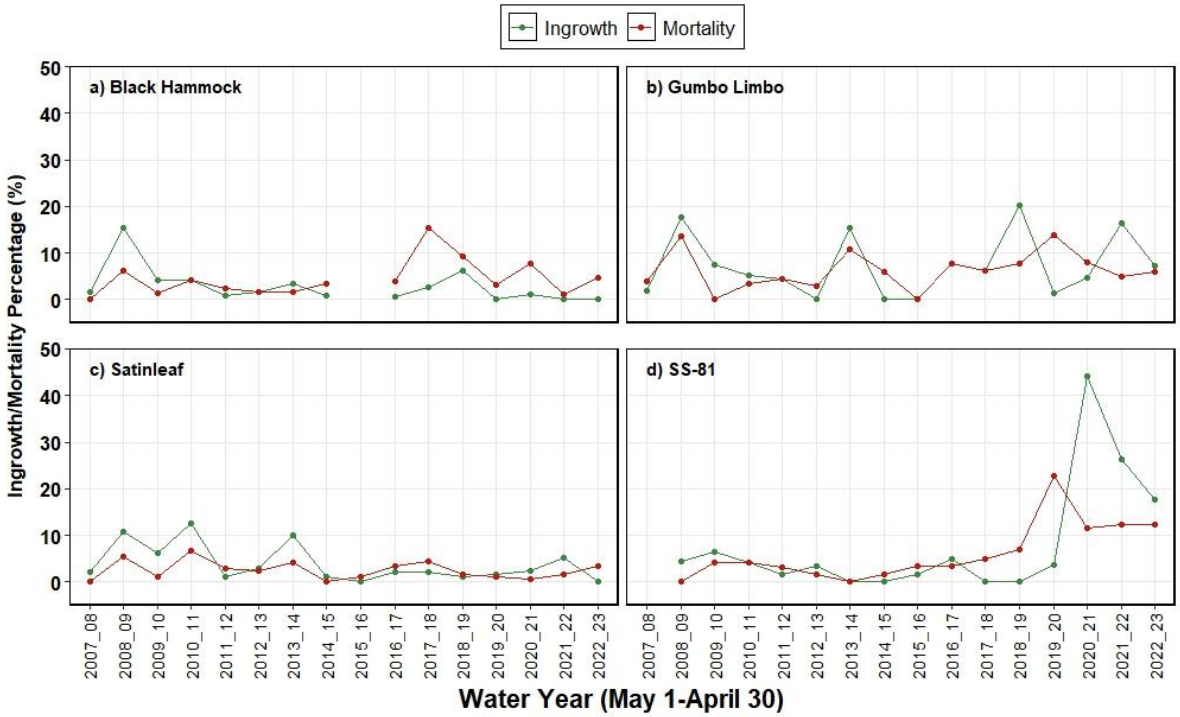

Figure 1.8: Annual mean (±) tree ingrowth and mortality on four tree islands annually monitored within the Everglades National Park between WY 2007/08 and 2022/23.

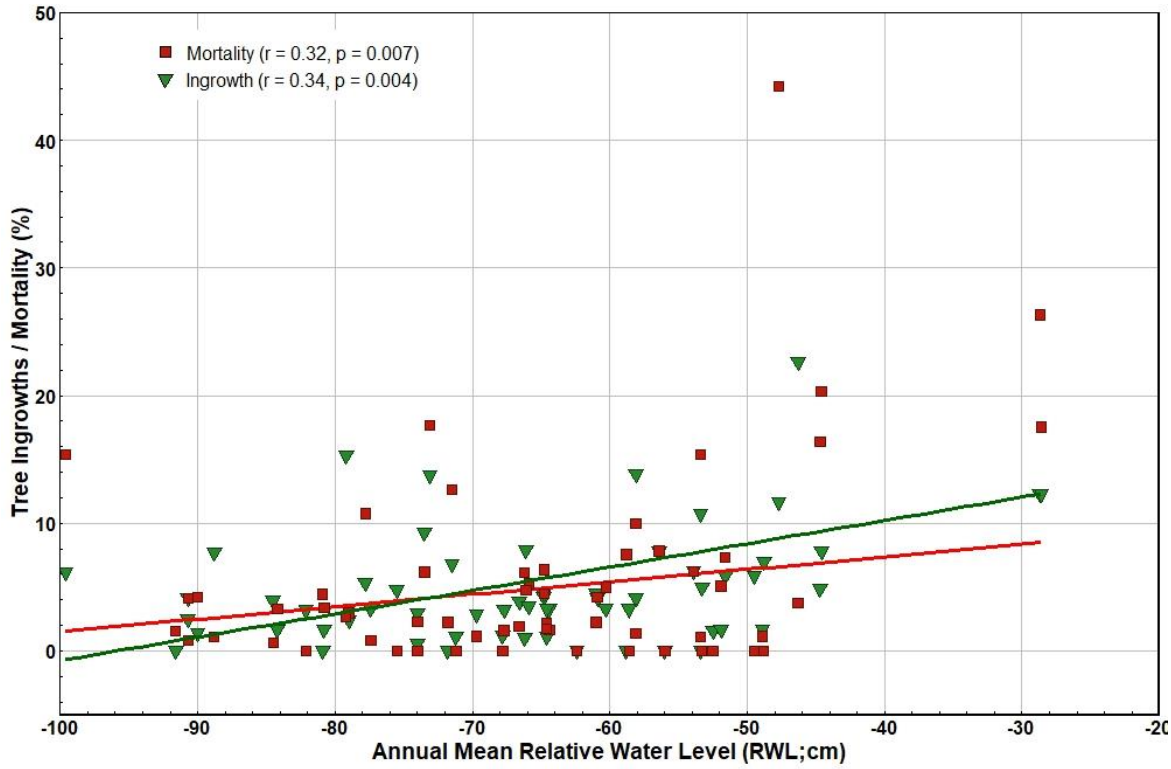

Figure 1.9 Scatterplot showing the relationship between annual mean relative water level (RWL) and tree ingrowth and mortality on four tree islands monitored within the Everglades National Park between WY 2007/08 and 2022/23.

In concurrence with the trend in tree mortality and ingrowth on four islands that were monitored in all years, total tree basal area first increased between WY 2007/08 and 2009/10 (r = 0.99, p = 0.058), and then significantly decreased over the next 13 years, between 2010/11 and 2022/23 (r = -0.66, p = 0.006; Figure 1.10). The lowest value of total BA in WY 2015/16 was because only three tree islands were sampled in that year. Black Hammock, which has higher (38% of total) BA than the other three islands, was not sampled in 2015/16. On these islands, a sharp decrease in BA was observed after 2017/18, as the total basal areas in post-Irma years was even lower than in 2006/07 (one year after Hurricane Wilma). In fact, mean basal area was significantly lower in post-Irma years (WY 2017/18 – 2022/23) than before the hurricane (2007/08 – 2016/17) on Black Hammock and Gumbo Limbo. However, basal areas have recovered in Satinleaf (Figure 1.11). On the other four islands, which were sampled only for three years after hurricane, the mean basal was higher on three of four islands in those years (2017/18 – 2019/20) than 7-10 years before Irma (i.e., 2007/08 – 2010/11) (Figure 1.10), suggesting that those islands were not much affected by the hurricane. In contrast, on vulture islands which had 65-80% trees damaged, the mean basal area in post-hurricane years was lower than 7-10 years ago (Figure 1.11).

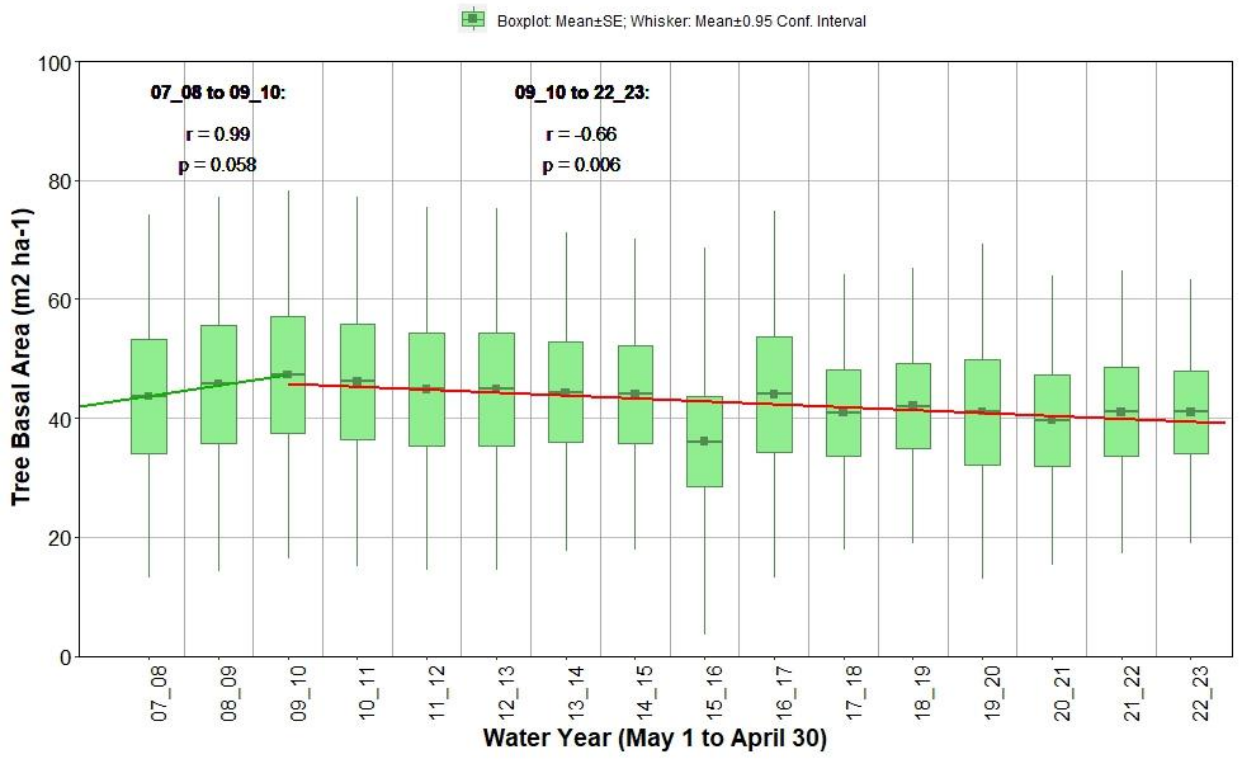

Figure 1.10: Boxplot showing the trend in tree basal area on four tree islands monitored within the Everglades National Park between WY 2007/08 and 2022/23). In WY 2015/16, tree basal area was low, as only three tree islands were sampled.

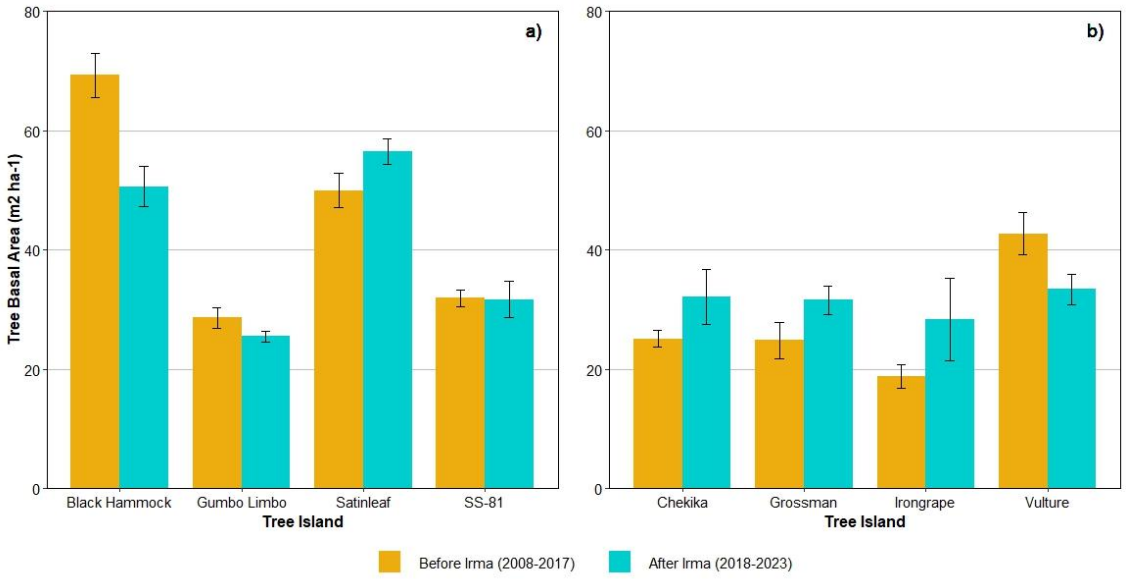

Figure 1.11 Bar diagram showing mean (± SD) tree basal area on eight tree islands monitored within the Everglades National Park before and after hurricane Irma. (a) Four islands were monitored annually since WY 2007/08, except in WY 2016, when only three islands were sampled. (b) Four other islands were sampled between WY 2007/08 and 2010/11 (before Irma), and then again for three years between WY 2017/18 and WY 2019/20.

A preliminary analysis of the relationship between RWL and BA revealed that across all the islands and years, basal area was negatively correlated with mean annual water level that were averaged over 1, 3 and 7 years prior to the sampling year (Table 1.3). However, the relationship of basal area with mean annual RWL differed among tree islands. Most islands showed significant relationships with hydrologic conditions one year prior to sampling, while only one island had a significant relationship between basal area and 7-year average RWL (Table 1.4). An in-depth analysis of the relationship between RWL and tree growth (change in basal area) is in progress and will be included in next year's report.

Table 1.3: Relationship between relative water level (RWL) and basal area (BA) on studied islands.

Tree Island	**N**	**RWL (1-year average)**		**RWL (3-year average)**		**RWL (7-year average)**	
		r	**p-value**	**r**	**p-value**	**r**	**p-value**
Black Hammock	17	-0.654	**0.004**	-0.702	**0.002**	-0.469	0.058
Chekika	9	0.856	**0.003**	0.641	**0.063**	0.224	0.562
Grossman	9	0.773	**0.015**	0.261	0.498	-0.016	0.968
Gumbo Limbo	18	-0.495	**0.037**	-0.695	**0.001**	-0.420	0.083
Irongrape	8	0.413	0.309	0.554	0.154	0.380	0.353
Satinleaf	18	0.566	**0.014**	0.193	0.444	-0.108	0.670
Heartleaf (SS-81)	16	0.154	0.569	0.070	0.797	0.015	0.955
Vulture	9	-0.411	0.271	-0.469	0.203	-0.678	**0.045**
All islands	**104**	-0.265	**0.007**	-0.314	**0.001**	-0.341	**0.000**

1.3.3 Tree layer vegetation dynamics

Among the eight islands, tree layer vegetation composition on Grossman and SS-81, located within the MP landscape and NESRS, respectively, was quite different from the SRS tree islands. A nonparametric multi-dimensional scaling (NMDS) ordination, based on tree species' importance value (IV) and B-C dissimilarity, revealed that tree species composition has changed slightly in the hammocks of these eight islands (Figure 1.12). Such changes were obvious on six islands (Black Hammock, Chekika, Gumbo Limbo, Irongrape, SS-81 and Vulture Hammock). Of these six islands, Gumbo Limbo, Chekika, Irongrape and SS-81 showed a distinct change in post-Irma years. The most dramatic change was in Irongrape, on which the vegetation composition in WY 2018/19 and 2019/20 were quite different from the vegetation in other years. (Figure 1.12). Among them, SS-81 also had a noticeable change in tree layer composition in the last three years, i.e., between 2020/21 and 2022/23.

Among the four islands sampled in 2022/23, three islands (Black Hammock, Gumbo Limbo and Satinleaf) did not show much difference in hardwood hammock tree layer vegetation from the previous two years. However, in those three years, a gradual shift in position of SS-81 in ordination space towards increasing wetness suggested noticeable changes in tree species composition driven by hydrologic changes within the area (Figure 1.12).

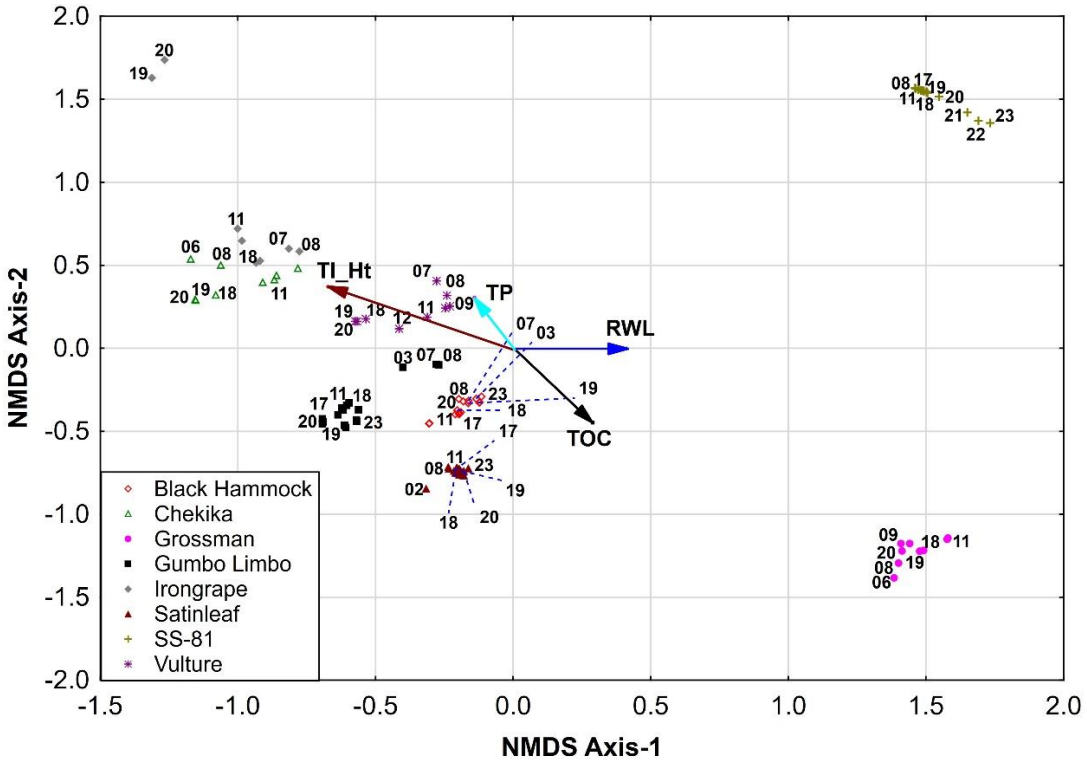

Figure 1.12 Scatterplot of NMDS ordination based on tree species IV in eight tree island hammocks sampled between Water Year (WY) 2001/02 and 2022/23. Fitted vectors are relative water level (RWL), tree island height (TI_Ht), soil phosphorus (TP) and total organic carbon (TOC). The plot includes the sites' position only in selected years, WY2002 & 2003 (when three islands were sampled for the first time), WY 2007 – 2011 (when all 8 islands were sampled, and WY 2018-2023 (all the post-Irma years).

On the tree islands, change in species composition was accompanied was mainly driven changed in their relative abundance. On Black Hammock, the IV of gumbo limbo (*Bursera simaruba*) and sugarberry (*Celtis laevigata*) decreased, whereas the IV of white stopper (*Eugenia axillaris*) increased significantly (Figure 1.13a). Likewise, the IV values of mastic (*Sideroxylon foetidissimum*) on Gumbo Limbo and of satinleaf (*Chrysophyllum oliviforme*) on Satinleaf islands, respectively, doubled in two decades, i.e., since the hardwood hammocks on those islands were first time sampled in 2001 and 2002 (Figure 1.13 b, c). The most significant change on Gumbo Limbo was the decrease in IV of *C. laevigata* (Figure 1.13b). Almost all individuals of this species were dead in 2019, and its IV decreased from 24.06% in WY 2007/08 to 1.05% in 2022/23. On these three islands, while there was not much shift in species composition between WY 2010/11 and 2016/17, there were some changes in composition after Hurricane Irma. After the hurricane, two species, Brazilian pepper (*Schinus terebinthifolia*), an invasive species, and lancewood (*Nectandra coriacea*), a native species, were observed for the first time on Gumbo Limbo (Figure 1.11b). In six years (from WY2017/18 to 2022/23), their IV values have increased from 1.0% to 3.7% and 2.0%, respectively.

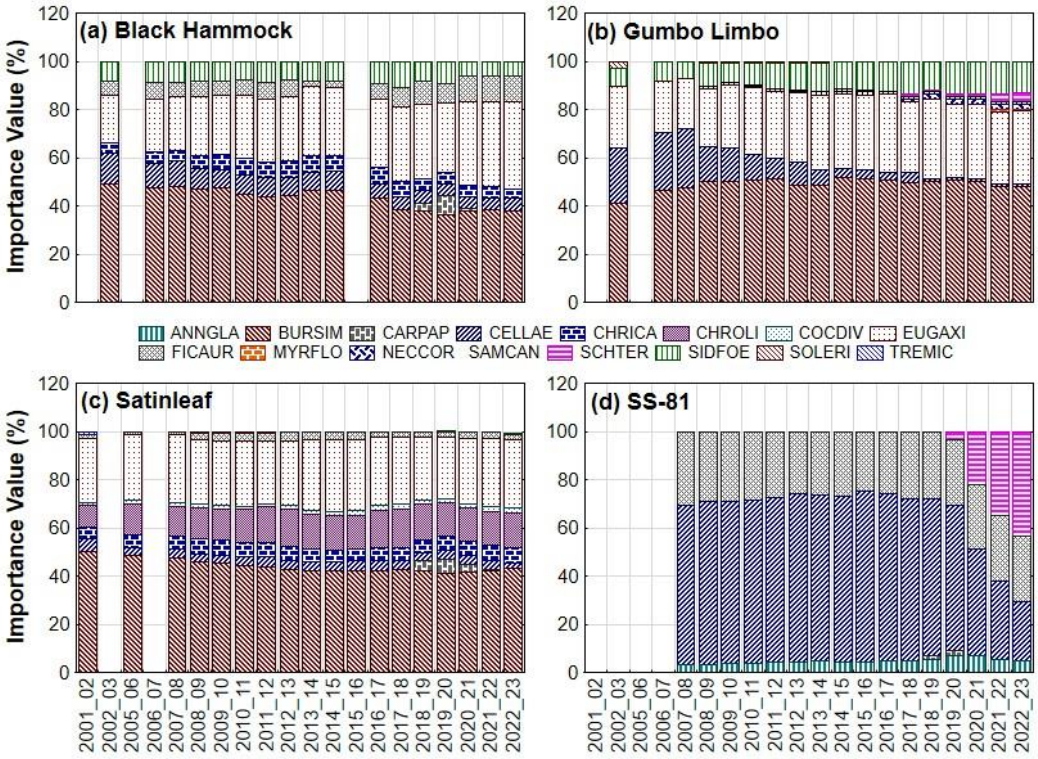

Figure 1.13 Importance value index (IV) of tree species in hardwood hammocks of four tree islands monitored annually. ANNGLA = *Annona glabra*; BURSIM = *Bursera simaruba*; CARPAP = *Carica papaya*; CELLAE = *Celtis laevigata*; CHRICA = *Chrysobalanus icaco*; CHROLI = *Chrysophyllum oliviforme*; COCDIV = *Coccoloba diversifolia*; EUGAXI = *Eugenia axillaris*; FICAUR = *Ficus aurea*; NECCOR = *Nectandra coriacea*: SAMCAN = *Sambucus canadensis*; SCHTER = *Schinus terebinthifolius*; SIDFOE = *Sideroxylon foetidissimum*; SOLERI = *Solanum erianthum*; TREMIC = *Trema micranthum.*

A significant shift in species composition in the tree layer was also observed in the hammock of SS-81, which has been monitored annually since WY 2007/08. On this island, the IV of sugarberry (*C. laevigata*) decreased from 66.3% in 2007/08 to 24.4% in 2022/23. A sharp decrease in its IV occurred after WY 2019/20 (Figure 1.13d). In contrast, IV of pond apple (*Annona glabra*) almost doubled in 13 years. Another significant change in vegetation composition included the appearance of Brazilian pepper, which was recorded for the first time on this island in WY 2019/20. Surprisingly, its IV values increased from 3.4% to 43.2% in four years, resulting in this species to be one of three dominant species in tree-layer vegetation of this this island. The distinct vegetation composition in the most recent three years (2019 to 2023) is also reflected in a shift in position of this island within the ordination space (Figure 1.12).

Hardwood hammocks on the other four islands (Chekika, Grossman, Irongrape and Vulture) were sampled annually until 2011/12, and then in 2017/18, 2018/19 and 2019/20. Among these, Grossman Hammock had relatively stable vegetation composition, whereas the other three islands showed a significant change in species abundances (Figure 1.14).

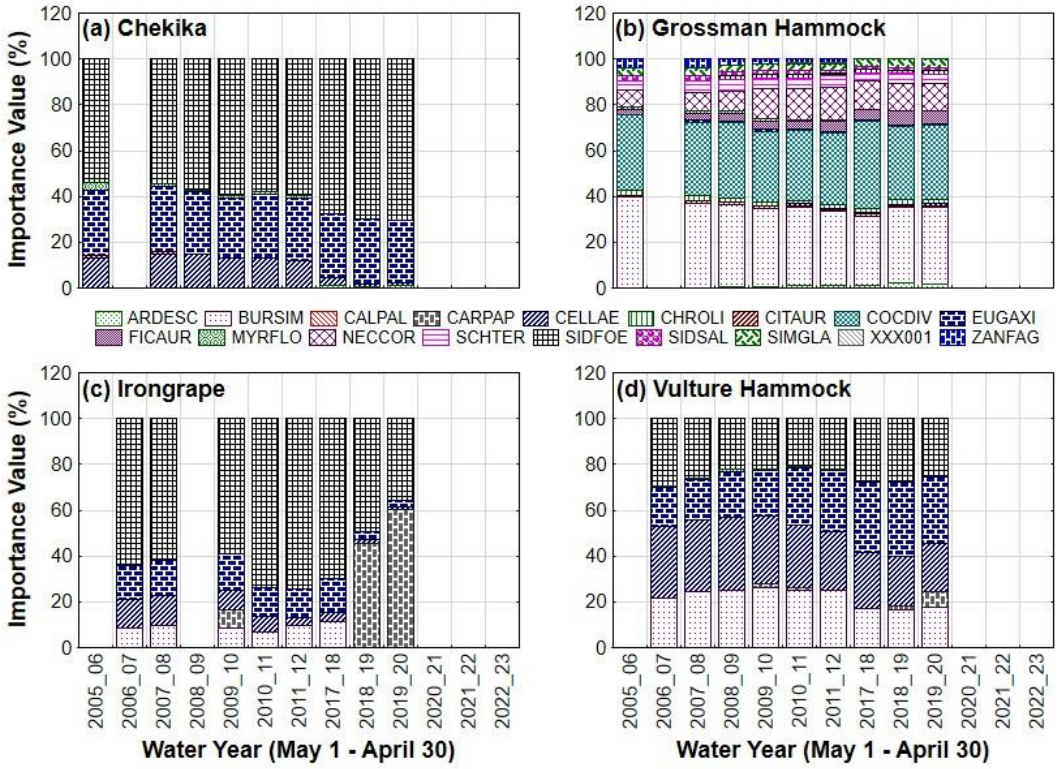

Figure 1.14 Importance value index (IV) of tree species in hardwood hammocks of four tree islands that were monitored until 2011/12, and then again in 2017/18, 2018/19, 2019/20. ARDESC = *Ardisia escallonioides*; BURSIM = *Bursera simaruba*; CALPAL = *Calyptranthes pallens*; CARPAP = *Carica papaya*; CELLAE = C*eltis laevigata*; CHROLI = *Chrysophyllum oliviforme*; CITAUR = *Citrus aurantifolia*; COCDIV = *Coccoloba diversifolia*; EUGAXI = *Eugenia axillaris*; FICAUR = *Ficus aurea*; MYRFLO = *Myrsine floridana*; NECCOR = *Nectandra coriacea*; SCHTER = *Schinus terebinthifolius*; SIDFOE = *Sideroxylon foetidissimum*; SIDSAL = *Sideroxylon salicifolium*; SIMGLA = *Simarouba glauca*; XXX001 = Unknown species; and ZANFAG = *Zanthoxylum fagara*.

One year after Hurricane Irma, the IV of sugarberry (*C. laevigata*) on Chekika was 1/10th of its IV in 2012, and the trend continued the following year (2019/20), i.e., two years after the hurricane (Figure 1.14 a). Similarly, on Vulture, IV of sugarberry (*C. laevigata*) was 33% less in post-Irma years than in 2012 (Figure 1.14 d). In contrast, mastic (*S. foetidissimum*) and white stopper (*E. axillaris*) increased on these two islands, respectively. Moreover, a major change was observed in tree layer species on Irongrape where papaya (*C. papaya*), a semi-woody ephemeral species, significantly increased after Hurricane Irma (Figure 1.14 c). In contrast, the abundance of all other major species declined in recent years. For instance, the number of trees of two species, gumbo limbo (*B. simaruba*) and mastic (*S. foetidissimum),* sharply declined in the post-Irma period. On Vulture Hammock, while *C. papaya* was recorded for the first time in 2019/20, after 9 years, the abundance of gumbo limbo (*B. simaruba*) and sugarberry (*C. laevigata*) declined by 33% and 40%, respectively (Figure 1.14 d). In contrast, the IV of white stopper (*E. axillaris*) has doubled in 14 years, from 2006/07 to 2019/20.

1.3.4 Herb and shrub layer vegetation dynamics

Like the tree layer, understory species composition on Grossman and SS-81 tree islands was also somewhat different from the understory vegetation on other islands (Figure 1.15). Moreover, the results of the NMDS ordination revealed that variation in understory species composition within an island over time was more divergent (Figure 1.15) than the tree layer species composition on the same island (Figure 1.12). As expected, such a shift in understory composition was noticeable in 2006/07 and/or between in 2017/18 and 2022/23 (i.e., after hurricane Wilma and Irma, respectively) on majority of islands, possibly due to hurricane-induced changes in canopy cover and light availability in the understory.

On the studied islands, total understory plant cover increased until 2-3 years after Hurricane Wilma primarily due to an increase in cover tree seedlings, and then started to decrease. In the understory of SRS islands, the tree seedlings of white stopper (*Eugenia axillaris*) reached high densities (Figure 1.16). In contrast, the understory on Grossman, an island within the MP landscape, had a high cover of lancewood (*Nectandra coriacea*) seedlings (Figure 1.17). In fact, the relationship between canopy cover (Canocov) with the ordination configuration was highly significant, reiterating that canopy cover affected understory composition in the hardwood hammocks of those islands over time (Table 1.4). In addition, the environmental vectors representing relative water level (RWL) and soil depth (SoilDep) were also significantly correlated with the ordination configuration.

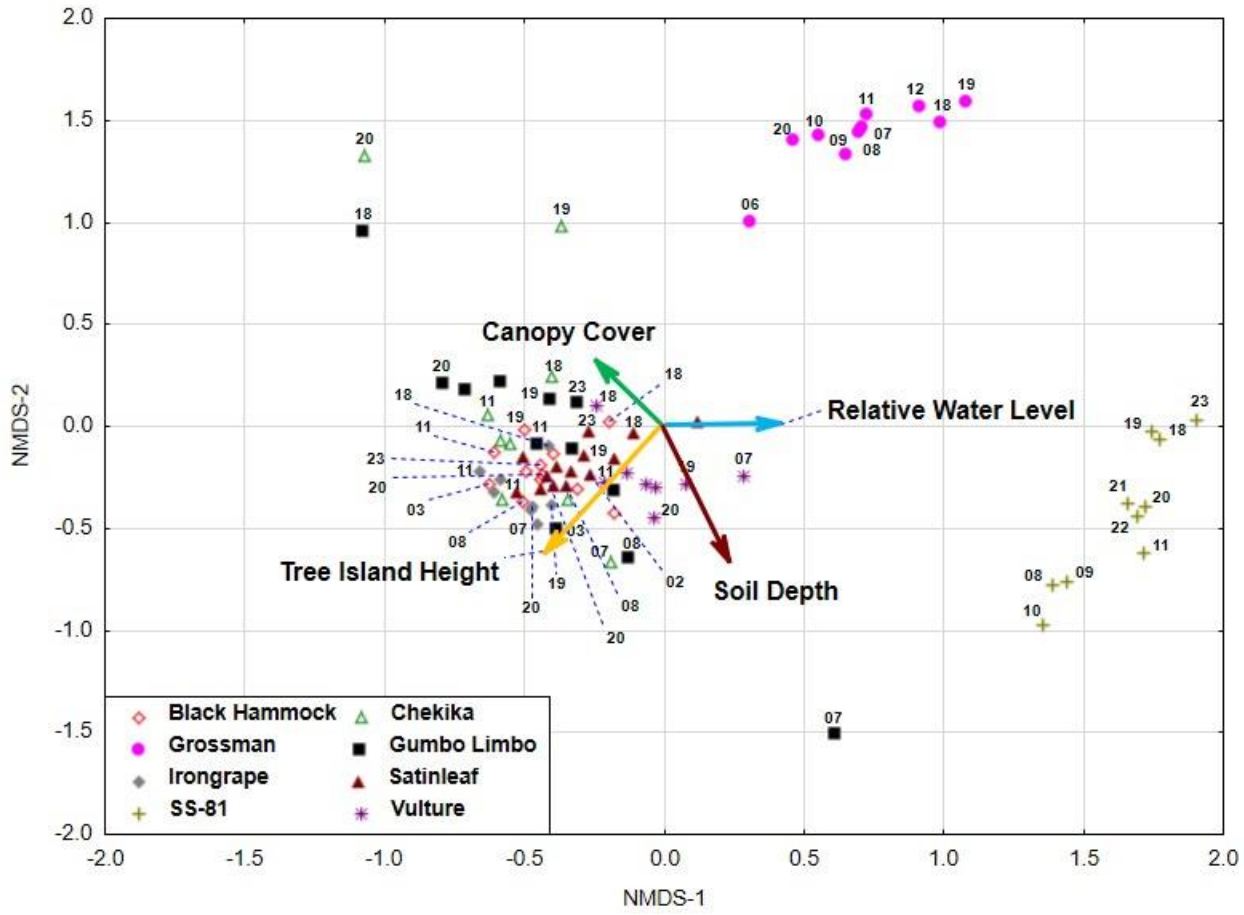

Figure 1.15 Scatterplot of NMDS ordination based on herb and shrub species cover on eight tree island hammocks sampled between Water Year (WY) 2001/02 and 2022/23. Fitted vectors are relative water level, canopy cover, tree island height and soil depth.

Table 1.4 Correlation (r) and statistical significance of fitted environmental vectors with species cover-based 2-dimensional non-metric multi-dimensional scaling (NMDS) ordination configuration.

Vectors	R^2	p-value
Relative water level	0.17	<0.001
Soil depth	0.50	<0.001
Canopy cover	0.15	0.002
Tree island height	0.56	<0.001

Total understory cover was low before Hurricane Irma. Thereafter, the understory cover increased again in the first year after Hurricane Irma on four of these five islands (Figures 1.16, 1.17). A noticeable increase in understory cover in 2019/20 was also observed on Chekika, mostly due to a 6-fold increase in fern (*Blechnum serrulatum*, *Nephrolepis biserrata*, and others) cover (Figure 1.17a). Fern percent cover significantly increased also on other two islands, Gumbo Limbo and SS-81. In contrast, on Gumbo Limbo, the cover of *Rivina humilis*, the most

dominant species in the understory during post-Wilma years on that island, has significantly decreased in recent years. Mean cover of *R. humilis* was 67.8% in 2007/08, but 1% in 2022/23 and the drastic drop in its IVI occurred between WY 2007/08 and 2008/09, i.e., 2-3 years after hurricane Wilma (Figure 1.16 b). In fact, this species was almost absent just before and after hurricane Irma. Thereafter, its IV greatly varied over the next six years.

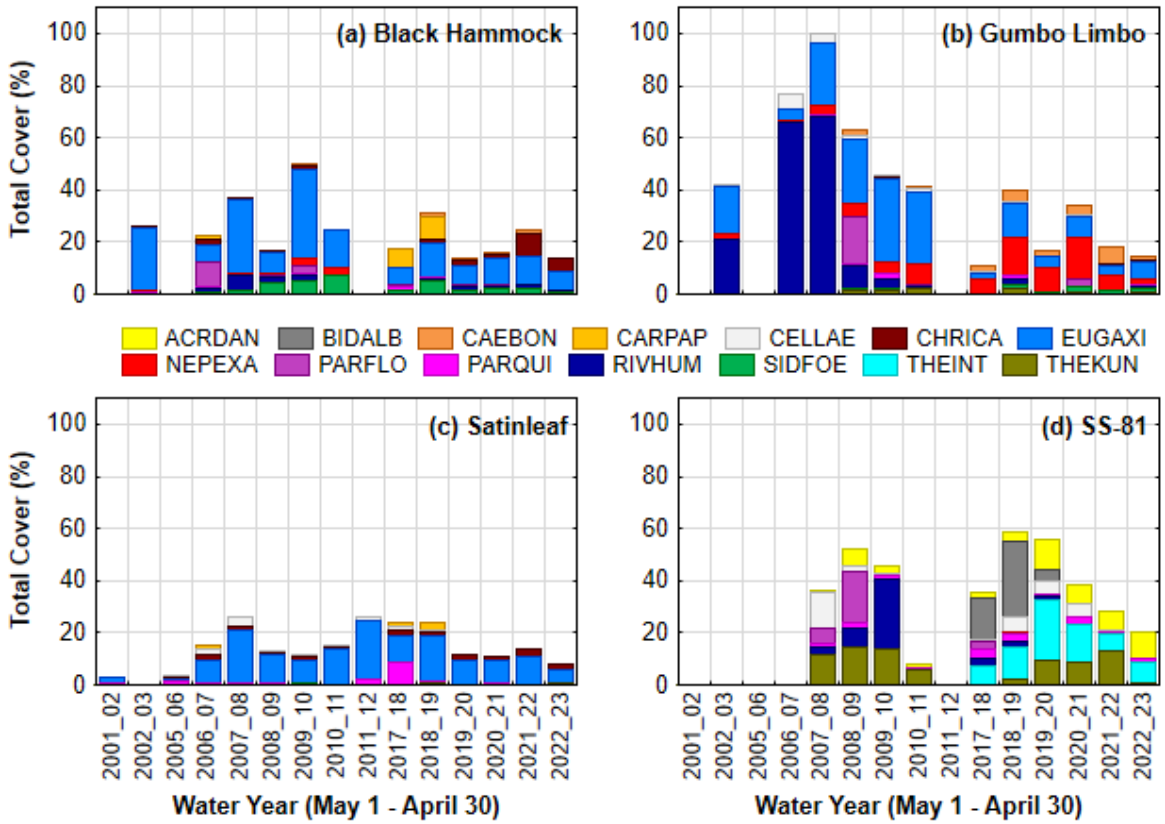

Figure 1.16 Percent cover of herb and shrub species in hardwood hammocks of four tree islands. ACRDAN = *Acrostichum danaeifolium*; BIDALB = *Bidens alba*; CAEBON = *Caesalpinia bonduc*; CARPAP = *Carica papaya*; CELLAE = *Celtis laevigata*; CHRICA= *Chrysobalanus icaco*; EUGAXI = *Eugenia axillaris*; NEPEXA= *Nephrolepis exaltata*; PARFLO= *Parietaria floridana*; PARQUI= *Parthenocissus quinquefolia*; RIVHUM= *Rivina humilis*; SIDFOE = *Sideroxylon foetidissimum*; THEINT = *Thelypteris interrupta*; THEKUN= *Thelypteris kunthii*.

The effects of canopy cover on the understory layer were much more distinct on Irongrape, which was relatively open 13 years ago. On this island, the total cover of all species in the understory was >100 %, mostly due to number of white stopper seedlings (Figure 1.17 c). But it now has a dense canopy due to both an increase in tree basal area (from 19.5 m^2 ha^{-1} in 2007 to 36.2 m^2 ha^{-1} in 2020) as well as an extensive growth of woody climber yellow nicker (*Caesalpinia bonduc*).

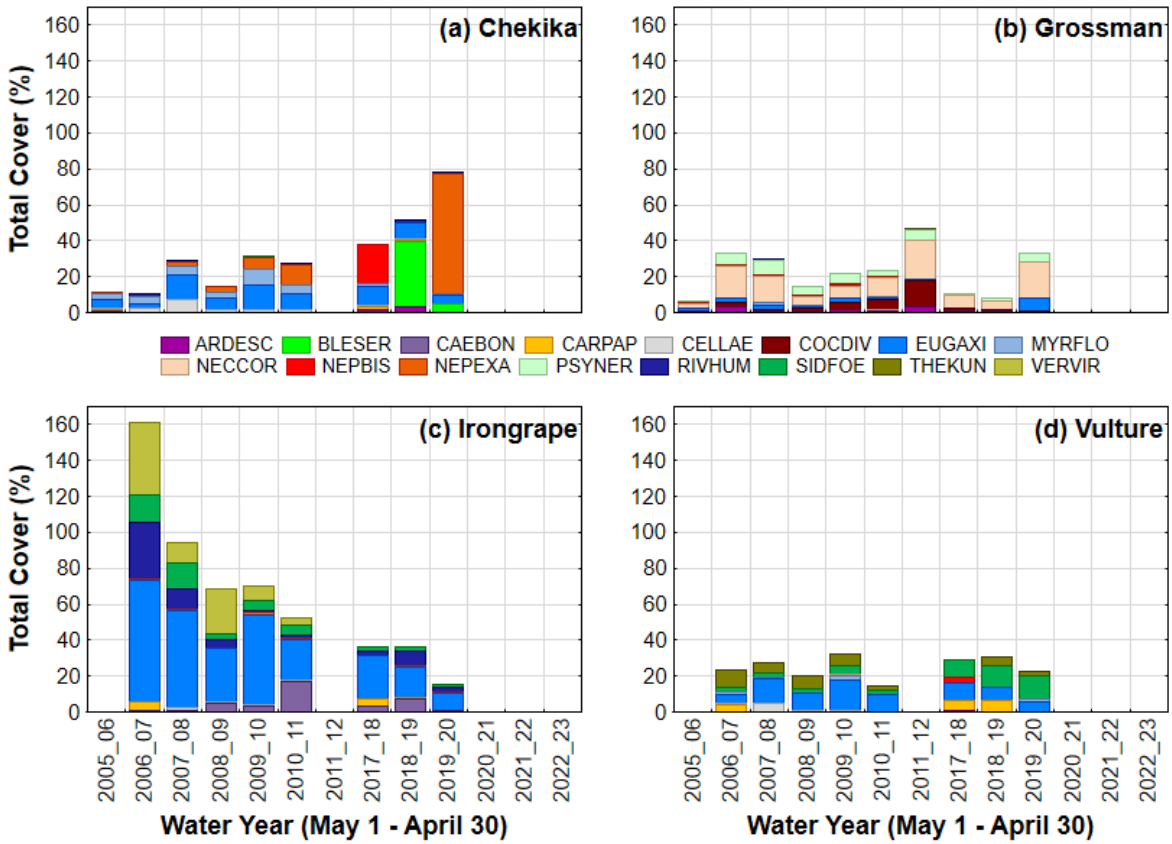

Figure 1.17 Percent cover of herb and shrub species in hardwood hammocks of four tree islands. ARDESC= *Ardisia escallonioides*; BLESER = *Blechnum serrulatum*; CAEBON= *Caesalpinia bonduc*; CARPAP= *Carica papaya*; CELLAE= *Celtis laevigata*; COCDIV= *Coccoloba diversifolia*; EUGAXI = *Eugenia axillaris*; MYRFLO = *Myrsine floridana*; NECCOR = *Nectandra coriacea*; NEPBIS = *Nephrolepis biserrata*; NEPEXA= *Nephrolepis exaltata*; PSYNER= *Psychotria nervosa*; RIVHUM= *Rivina humilis*; SIDFOE = *Sideroxylon foetidissimum*; THEKUN= *Thelypteris kunthii*; VERVIR= *Verbesina virginica*.

1.4 Discussion

In the Everglades, in the hardwood hammock portions of tree islands that we studied, plant communities respond to changes in hydrologic conditions and the periodic disturbances such as tropical storms. Our results show that rising water level and periodic fluxes in the hydrologic regime directly and/or interacting with tropical storms affect the tree demography and both the tree layer and understory (herb and shrub) vegetation composition. However, their effects vary among islands depending on the position of islands within the landscape and existing hydrologic conditions.

In WY 2022/23, hydrologic conditions at the studied tree islands were wetter than previous years on all islands. In fact, annual mean water levels in these tree islands in WY 2022/23 were 14.2 to 33.5 cm above the 32-year (WY 1991/92 – 2022/23) average (Figure 1.2). One tree island in NESRS region, which is experiencing increasing wetness driven by increased water delivery into ENP, had the highest RWL in last 17 years. On this island, the mean water level in 2022/23 was within 25 cm below the ground surface and 33% of the vegetation monitoring plot (300 m^2) was flooded >50 days. High water level in studied islands in WY 2022/23 were due to both high rainfall in the Everglades basin and increased inflow into ENP (Cortez, 2024). For instance, within the SFWMD basin, WY 2022/23 had total annual rainfall of 1,405 mm (55.3 inches), i.e., 54 mm (2.11 inches) more rain than the historical 30-year (1991-2020) average. In WY 2022/23, the total inflow into ENP was 162% of the historical flow averaged over 48 years (1972-2019). Likewise, within the SRS, the average stage at P-33 was 211.8 cm (6.95 ft), which was 9.14 cm (0.3 ft) and 26.5 cm (0.87 ft) higher than the stage in WY 2021/22 and long-term (70 years: 1952-2022) average, respectively (Cortez, 2024).

Hydrologic condition in tree island hammocks varies depending on the location of tree islands within the R&S landscape and tree island height above the surrounding marshes. Based on their locations, islands in the NESRS area had been drier than the western and central SRS islands and might be expected to have the lowest water level below the ground. However, while our results showed that Chekika had the lowest RWL, not all islands in NESRS had a lower RWL than islands in other regions. For instance, SS-81, located downstream of the 1-mile Tamiami Bridge, had relatively low water level until 2015, but thereafter RWL on that island has been consistently high (Figure 1.3). On that island, the relatively high-water level in recent years is primarily because of water deliveries into ENP under the Increment Field Tests associated with the Combined Operational Plan (COP) that took place between 2015 and 2019, followed by its implementation thereafter (*see the next paragraph*). Due to an increase in water deliveries into ENP in recent years, water level even in Chekika island, also within the NESRS region, was higher than long-term average, in every single year since WY 2017/18 (Figure 1.3), and it was more than 20 cm since WY 2020/21, i.e., the year when operations under COP was fully implemented. Moreover, hydrologic conditions on tree islands are not simply the function of regional marsh hydrology but could also be a function of the geomorphological characteristics of tree islands, such as the tree island height – the difference in elevation between the surface of the

tree island and the surrounding marsh. In a study of 76 slough and prairie tree islands within ENP and WCA3B, RWL was negatively correlated with tree island height (Ross and Sah, 2011). Among the eight islands studied, Chekika and Vulture had lower RWL than other islands and had also the greatest tree island height (Table 1.1).

In the hardwood hammocks of the most of studied islands, the annual mean RWL remained well below the soil surface, suggesting that limited increase in marsh hydroperiod or water depth in ENP are unlikely to have an immediate significant adverse impact on tropical hardwood hammock communities on these islands. An exception is SS-81 in NESRS on which sustained high annual mortality of sugarberry (*Celtis laevigata*), which has been characterized as shallow-rooted (Kennedy 1990) and weakly to moderately flood-tolerant (Hook 1994), in the last four years needs more attention. This is important, especially when, as outlined in the Central Everglades Planning Project (CEPP) and Combined Operational Plan (COP), restoration activities are expected to further increase water deliveries from WCA 3A into ENP through NESRS (USACE, 2014, 2020). In fact, after the implementation of COP in August 2020, the volume of water delivered to NESRS across Tamiami Trail in WY2021 and 2022, was 71.0% and 84.6% higher than the volume delivered in WY2020 (USACE, ENP and SFWMD 2023). These changes in water deliveries are likely to affect vegetation composition on the tree islands in ENP. Using modeled water surface elevations for different scenarios described in CEPP, relative water level on tree islands in Western/Central SRS and NESRS was expected to increase by 5-10 cm and 15-20 cm, respectively (Wetzel et al., 2017). Despite model predictions of relatively wet conditions in SRS and NESRS in different restoration scenarios compared to current conditions, vegetation succession models using the Everglades Landscape Vegetation Succession (ELVeS) showed minimal or no change in plant community types on those islands (Wetzel et al., 2017).

Water conditions throughout the Everglades, including ENP, depend on the gradual implementation of restoration plan components. Under the preferred plan (ALTQ+) identified in the COP, water delivery into ENP (both northeast and western SRS combined) is projected to increase by 25%, resulting in an increase in water delivery into NESRS by approximately 162,000 acre-feet per year on average (USACE, 2020). Similarly, during the process of revisions to the 2005 Interim Goals and Targets for CERP, out of four simulations, the 2032PACR simulation projects the flow into NESRS to increase by a total of 528,000 acre-feet per year (RECOVER, 2020). In fact, water level in NESRS has already been relatively high because of the increased water delivery due to Increment Field Tests that began in October 2015 and continued through 2019 (USACE, 2020), followed by the implementation of the Plan in August 2020. In comparison to the WY 2015/16, when the Increment Field Tests began, the mean annual water levels in 2022/23 are already 31.8 cm and 33.7 cm high on Chekika island and SS-81, respectively.

After an analysis of possible inundation of 36 tree islands for which elevation data were available, it has been concluded that none of those islands will be inundated more than 10% of

the modeled time period, a performance indicator used to evaluate the Interim Goals scenarios (RECOVER, 2020; USACE, 2020), and thus may not have a drastic change in vegetation composition. However, an incremental upward shift in the RWL overtime could cause a shift in species composition and productivity of plant communities on these islands. Such a shift in vegetation in response to hydrologic change commonly occurred in wetter communities (bayhead and bayhead swamp) (Sah et al., 2018). However, a sharp decrease in tree density and basal area of flood-intolerant species sugarberry (*Celtis laevigata*) since WY 2014/15 (density and basal area by decreased by 69% and 59%, respectively) and an increase in abundance of flood-tolerant pond apple (*Annona glabra*) observed in hardwood hammock of the SS-81 island in recent years could be evidence of the effects of increased wetness in NESRS. Moreover, there was a dramatic increase in the number of Brazilian pepper (*Schinus terebinthifolia*) which was recorded on this island in WY 2019/20 for the first time.

In general, hydrology is the major driver of differences in species composition among various plant communities arranged along topographic gradients within a tree island (Armentano et al., 2002; Wetzel, 2002; Ross & Jones, 2004; Espinar et al., 2011; Sah et al., 2018). However, in the hardwood hammocks which rarely get flooded, and where the mean annual water table is often 40 cm or more below the ground surface, except in Grossman Hammock and SS-81 (Table 2; Figure 1.3), tree species composition dynamics is probably more the legacy of the long-term interaction between hydrology and other physical processes, including recurrent disturbances. On some of these islands, high tree mortality was observed until 3-4 years after Hurricane Wilma in 2005, and the delayed tree mortality in post-Wilma years was attributed to the interaction of multiple disturbances, e.g., hurricane and drought (Ruiz et al., 2011). Immediately after Hurricane Irma, we also observed severe damage to the tree layer vegetation on some of the islands for which we had pre-Irma data. Tree mortality after the hurricane was higher than the background mortality, i.e., mortality before the hurricane (Sah et al., 2020, 2021, 2022). In addition, like the trend observed after Hurricane Wilma (Ruiz et al., 2011), delayed mortality was observed on 4 of eight islands (Grossman, Gumbo Limbo, SS-81, and Vulture). On SS-81, tree mortality was four times higher in the two years than immediately after the hurricane, and more than five times higher than the background mortality. However, while post-Irma mortality stabilized in other islands, tree mortality on SS-81 remained high, though lower than two years post-Irma. As a result of tree mortality caused by the hurricane, as well as an unusual increase in ingrowths, a shift in vegetation composition was noticed on some of the studied islands (Figure 1.12).

In post-Irma years, i.e., since WY 2017/18, much obvious change in species composition was observed on Gumbo Limbo, Irongrape and SS-81. On Gumbo Limbo most of the sugarberry (*Celtis laevigata*) trees died, while on Irongrape and SS-81, it was the combination of increase in mortality of existing trees and an ingrowth of other species. On Irongrape, where the hardwood hammock was relatively open and very few hardwood trees were present up to 2010 (Ruiz et al., 2011), there was an increase in abundance of a naturalized form of a cultivated species, *Carica papaya*. The change in *C. papaya* itself may not indicate much about the health of the island, but

how the increased abundance of *C. papaya* would affect the germination and growth of the seedings of those hardwood species needs detailed analysis of seedling dynamics. On SS-81, a drastic change in vegetation composition, observed in WY 2019/20 and thereafter, was primarily due to a decrease in IV of moderately flood-intolerant species, sugarberry (*C. laevigata*) and an increase in IV of pond apple (*A. glabra*) and Braizilian pepper (*S. terebinthifolia*) possibly a result of combination of post-hurricane mortality and an increase in water level in NESRS or solely increased water level, respectively.

Trees on hardwood hammocks are primarily flood-intolerant species. Water level above or near the ground surface for longer periods, especially during the dry season, adversely impacts the survival and growth of those tree species (Stoffella et al., 2010). During the 2016 dry season, water level on the SRS tree islands was higher than that in the wet season and was very close (<40 cm) to the ground surface, i.e., in the root sensitive zone, for a longer period (Figure 1.4) than during other years, which may have affected tree growth and increased mortality in subsequent years. In this study, however, the RWL estimates are based on a flat-water table at the same elevation as in the marsh for which the EDEN estimates are derived. However, studies have suggested that the water table under the tree island can be drawn down further during the dry season and mounded during the wet season (Sullivan et al., 2010). Thus, the water level may not be flat throughout the year as assumed, but this assumption is useful to have an approximate estimate.

Brazilian pepper (*Schinus terebinthifolia*), an exotic invasive tree species in the Everglades, has been present in Grossman Hammock since we first studied the island in 2005/06. The presence of Brazilian pepper in this location is unsurprising, as the island is in a region of wildland-urban interface (WUI) in proximity to the eastern boundary of ENP. However, the species was recorded on Gumbo Limbo and SS-81 for the first time in 2017/18 and 2019/20, respectively. While its IV in the former was approximately 3.7% in WY2022/23, four times increase in its IV since 2017/18, the most remarkable change in abundance of this species occurred in SS-81, where its IV was only 3.4% in 2019/20, but increased by more than twelve-fold by 2022/23. Increase in Brazilian pepper abundance on SS-81 within such a short period is alarming. In fact, different aspects of the recent appearance and expansion of this species on ENP tree islands need to be carefully and regularly monitored. Animals, including mammals, are the species' main dispersers (Ewel et al., 1982). However, Brazilian pepper seeds can be dispersed as much as 10-15 km in fresh or brackish water (Tassin et al., 2007; Donnelly and Walters 2008). Thus, the water flowing from the north into NESRS, which has resulted in increased water level and partial flooding of the SS-81 hardwood hammock for varying periods, may have contributed to the dispersal of Brazilian pepper into this island. A timely eradication of this exotic species would be desirable.

Other studied islands also experienced relatively high mortality in post-Irma years (Figure 1.7). However, those islands together with thirty other SRS islands are not expected to experience flooding more than 10% of the year, even in the preferred scenario of Combined

Operational Plan (USACE 2020). Nonetheless, since some islands, especially Black Hammock, Chekika and Irongrape, are in the path of water flow through NESRS, an increase in their water levels is expected to be steeper than in other parts of SRS. The response of NESRS islands therefore requires care and regular monitoring to establish an effective link between science and management.

Beside water level and windstorms, fire is another stressor that affects tree island vegetation, especially when it consumes peat soils and lowers surface elevation (Wetzel et al., 2008). On our studied islands, hardwood hammocks had not been burned between 2001 and 2023. However, a fire in 2008 had burned up to close to the hardwood hammock on Black Hammock, affecting the boundary between the tree island and surrounding marsh (Sah et al., 2018). Thus, the observed dynamics of plant communities in the hardwood hammocks were primarily the result of hydrologic changes and impact of tropical storms.

In summary, community dynamics in the hardwood hammock portions of the study islands, which are rarely flooded and have not burned for decades or more, tree species composition is primarily the legacy of the long-term interaction between hydrology and tropical storms, though short-term responses in tree demography or understory species composition may result from flooding events and/or tropical storms. In addition, recent records of high mortality of flood-intolerant species and an invasive species on two islands suggesting the expansion of its range within ENP need additional attention. Especially, the islands, e.g., SS-81 in NESRS, that are being impacted by increasing water levels driven by incremental water delivery into ENP, need special care, including early eradication of the exotic species.

2. Plant Community Distribution on Tree Islands in ENP

- Ximena Mesa and Daniel Gann

2.1 Introduction

Tree island monitoring is an essential aspect of the implementation of the Comprehensive Everglades Restoration Plan (CERP), to assess the impact of hydrological regime shifts on tree island vegetation composition, structure, and island configuration. To understand how the structure and composition of plant communities in tree islands are correlated and respond to hydrologic regimes and their change, we developed a mapping method that allows us to detect and model structural vegetation community classes from very high-resolution multi-spectral satellite data in combination with Light Detection and Ranging (LiDAR) derived canopy height and canopy structure metrics. Accurate detection of plant communities at a resolution that represents the scales at which change is expected to occur along hydrologic and nutrient gradients had previously been demonstrated for nine tree islands mapped between 2014 and 2023 (Sah et al., 2020). At the time the mapping method of Gumbo Limbo and NP-202 did not include a canopy height source and Irongrape and Vulture were mapped using uni-season data only.

The objective of this iteration was to standardize and apply the optimized detection method and apply the algorithms to map the baseline community classes of ten tree islands located in the Shark River Slough and one tree island in the marl prairies in Everglades National Park (ENP), using bi-season multispectral satellite data with LiDAR data derived canopy structure metrics. We then analyzed and modeled the woody community distribution across all eleven islands to determine if the percent cover of each woody class on islands is correlated with the size of the total woody core area that encompasses the three woody classes Hardwood Hammock, Bayhead trees and Bayhead shrubs.

2.2 Methods

2.2.1 Study Area

The eleven tree islands we mapped included five islands (Black Hammock, Gumbo Limbo, Satinleaf, Vulture, and NP-202) in Shark River Slough; five (Chekika, Irongrape, SS-81, SS-93, and SS-94) in Northeast Shark River Slough; and one prairie island (Grossman Hammock) along the eastern border of ENP (Figure 2.1 and Table 2.1). For each island type, we defined a classification schema that best represents the vegetation classes of woody vegetation and adjacent marsh or prairie communities (Table 2.2). Tree island vegetation classes included hardwood hammock (tH) with trees or woody species with heights greater than 5m that are not typically found in standing water, bayhead forest (tB) with trees or woody species, and bayhead swamp representing shrubs, or woody species less than 5 m tall (sB). A mixed broadleaved emergent class with low shrubs, typically found in tree island tails and edges frequently included *Cephalanthus occidentalis* (buttonbush) and/or fern species and broadleaved emergent species with strong graminoid presence (typically sawgrass) (hV_s).

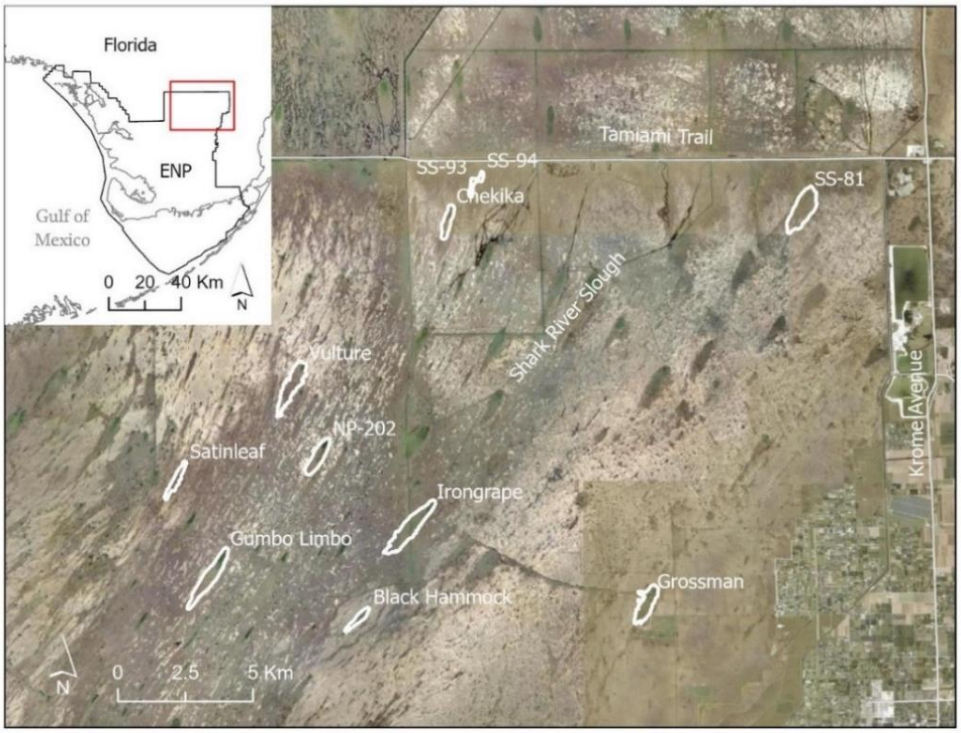

Figure 2.1 Location of the eleven tree islands. Black Hammock, Gumbo Limbo, Satinleaf, Vulture and NP-202 are in the central Shark River Slough; Chekika, Irongrape, SS-81, SS-93, and SS-94) in Northeast Shark River Slough; and Grossman Hammock is in the marl prairie along the eastern border of ENP.

Table 2.1 Approximate location of the highest location of the woody vegetation of each island.

Tree Island	Easting (UTM 17N)	Northing (UTM 17N)
NP-202	529789	2838868
SS-93	535509	2848796
SS-94	533508	2848749
Black Hammock	531295	2832631
Chekika	534372	2847486
Grossman	541819	2833206
Gumbo Limbo	525999	2834794
Irongrape	533651	2836524
Satinleaf	524499	2838020
Heartleaf (SS-81)	547639	2848114
Vulture	528918	2841668

Marsh classes were divided into classes dominated by a single species or a mix of species. The dominant marsh classes included regular to dense graminoid marshes dominated by *Cladium jamaicense* (gMCl), or *Typha domingensis* (gMTy). Two mixed classes included a generic open marsh class with a mixture of submerged and floating vegetation including periphyton and sparse *Eleocharis spp.*, *Panicum spp.*, or *Rhynchospora spp.*, typically found in deeper and longer hydroperiod marshes or sloughs (oM) and a graminoid class of dense to very dense graminoid species dominated marsh (gM). A graminoid prairie class (gP) and a *Cladium*

dominated prairie class (gPCl) were included for Grossman Hammock, the only marl prairie island (Table 2.2).

Table 2.2 Vegetation class code and corresponding class descriptions

Class Code	Class Name (Description)
oM	Open marsh (mixed species of floating and submerged
gM	Graminoid Marsh (mixed species of dense graminoid species
gMT	Graminoid Marsh Tall (mix of *Cladium* / *Typha*)
gMCl	Graminoid Marsh dominated by *Cladium jamaicense*
gMTy	Graminoid Marsh dominated by *Typha*
gP	Graminoid Prairie dominated by herbaceous vegetation
gPCl	Graminoid Prairie dominated by *Cladiu*m
hV_s	Mixed shrub, graminoid, and emergent broadleaf, including ferns
sB	Bayhead Shrubs dominated by woody species with heights less than 4 m
tB	Bayhead Trees dominated by woody species at least 4 m tall
tH	Hardwood Hammock
Wtr	Open Water

2.2.2 Data Selection and Processing

We chose WorldView (WV) 2 and 3 data to map the tree island plant communities because WV sensors have a very high 2 m spatial and eight spectral bands that were previously successfully used to detect wetland plant communities including woody vegetation (Gann, 2018; Gann & Richards, 2023; Hochmair et al., 2022; Sah et al., 2020; Wendelberger et al., 2018). Gann (2018) and Wendelberger et al., (2018) showed that bi-season data increased mapping accuracies significantly. The inclusion of airborne LiDAR data products further improved the detection accuracies of woody vegetation (Sah et al., 2020; Wendelberger et al., 2018).

The main criterium for WV data scene selection was the ENP LiDAR acquisition date of spring 2017. Our WV data scenes were optimally selected within less than five years of the spectral data acquisition. Images with minimal cloud cover were obtained for wet and dry conditions during the dry season, ranging from October to February and March to April, respectively. Optimally, the two dates were far enough apart to capture the highest variability of phenology of the vegetation while cloud cover was minimal during the dry season (late-October to mid-May). We mapped Black Hammock, Irongrape, NP-202, Vulture, Chekika, SS-93 and SS-94 from two images containing the seven islands that were obtained for the wet condition in 2018 (2018-02-16) and dry season in 2020 (2020-03-28). Three islands Gumbo Limbo, Satinleaf and Vulture were mapped from two images obtained on the wet condition of 2018 (2018-02-16) and dry condition of 2018 (2018-04-17). Two islands Heartleaf (SS-81) and Grossman Hammock were mapped from two images obtained in the wet condition of 2018 (2018-02-16) and on the dry condition of 2017 (2017-05-07). Vegetation in the last two islands was mapped independently from one another but still used the same images because of difference in vegetation communities between both tree islands.

The WV images were first geometrically, then radiometrically calibrated and atmospherically corrected in ENVI (*Exelis Visual Information Solutions*, 2013). Atmospheric

correction for the image was completed using the Fast Line-of-sight Atmospheric Analysis of Hypercubes (FLAASH) module in ENVI (ENVI, 2009). Selection of the atmospheric model used in FLAASH was based on local air temperature at the time of image acquisition while the aerosol model chosen was based on wind direction (coastal vs. inland) and time of year. In addition to the eight original spectral bands, we generated eight vegetation indices (VI) derived from WV2 spectral bands (Table 2.3).

Table 2.3 List of the eight vegetation indices (VIs) derived from WV imagery. Band wavelengths of WV-2: B1: Coastal Blue (400-450 nm), B2: Blue (450-510 nm), B3: Green (510-580 nm), B4: Yellow (585-625 nm), B5: Red (630-690 nm), B6: Red-edge (RE) (705-745 nm), B7: Near-infrared1 (NIR1) (770-895 nm), B8: NIR2 (860-1040 nm).

Vegetation Index	Acronyms	WV band wavelengths	References
Normalized Difference Vegetation Index	NDVI	(NIR1 - Red) / (NIR1 + Red)	(Rouse et al., 1974)
Normalized Difference Red-Edge Index	NDRE	(NIR1 - RE) / (NIR1 + RE)	(Barnes et al., 2000)
Normalized Difference Water Index	NDWI	(Green - NIR2) / (Green +NIR2)	(McFeeters, 1996)
Green Normalized Difference Vegetation Index	GNDVI	(NIR1 - Green) / (NIR1 + Green)	(Gitelson et al., 1996)
Enhanced Vegetation Index-2	EVI-2	2.5(NIR - Red) / (NIR1 + 2.4 Red +1)	(Jiang et al., 2008)
Normalized Difference Index using Red and Red-edge	NDI45	(RE - Red) / (RE + Red)	(Delegido et al., 2011)
Modified Chlorophyll Absorption in Reflectance Index	MCARI	1.2[2.5(NIR1 − Red) – 1.3(NIR1 − Green)]	(Daughtry et al., 2000)
Soil Adjusted Vegetation Index	SAVI	(1+L) (NIR1 - Red) / (NIR1 + Red + L) L = 0.5 in most conditions	(Huete, 1988)

Vegetation height and canopy structure information were represented with seven LiDAR-derived metrics for each WV pixel that were generated from the 2017 ENP LiDAR data point clouds. The LiDAR derived metrics included canopy pseudo-height (full range maximum –

minimum of LiDAR returns), lower and upper 25th and 50th percentile ranges, and their ratios. The resulting data cube had 31 layers or variables.

In a final step of data cube preparation, we masked previously digitized man-made structures on the islands and clipped the extent of the study area defined by a 200 m buffer of the approximate boundaries of each tree island that were manually digitized from high-resolution aerial photography in ArcGIS. The buffer of 200 m was generated to include the ecotone between the tree island and surrounding marsh communities and to allow for analysis of expansion and contraction of the tree islands over time.

2.2.3 Spectral Signature Evaluation

We evaluated the spectral signatures for each plant community of interest using a supervised classification algorithm. of vegetation classes training points were digitized across all islands representing all vegetation classes. Training samples for each vegetation class were digitized in ArcGIS using a combination of field surveys (2009) and high-resolution CIR aerial photography as reference. For all training samples, spectral signatures and LiDAR metrics were extracted from the 24-layer data cube. A random forest classifier (Breiman, 2001) as implemented in the unifying modeling framework of the 'caret' package (Kuhn, 2015) was trained. We determined from test runs that 500 decision trees were sufficient to maximize model-based classification accuracy, beyond which no significant increase in accuracy was observed ($\alpha = 0.05$) (Kuhn et al., 2015, 2019). The parameter for the optimal number of random variables selected at each split ("mtry") was established for each random forest model through built-in tuning routines.

2.2.4 Morphological Filtering of Vegetation Maps

The random forest model was applied to all pixels of the study area to generate the vegetation class map. A minimal mapping unit (MMU) of 12 m^2 was enforced for all classes by assigning a unique number to each connected region evaluating connectivity for the four nearest neighbors of each pixel and grouping pixels with the same value. Regions with an area equal to or below 12 m^2 were set to null and used as a mask to replace values with the values of the nearest neighbor from the original vegetation map.

2.2.5 User-Based Accuracy Assessment

We assessed the accuracy of the final plant community maps per image and separately for Heartleaf and Grossman (wet/dry: 2018/2018, 2018/2020, 2018/2017) using a stratified random sample design. The number of samples required was calculated assuming a multinomial distribution of error for a desired map accuracy confidence of 95% with a 5% precision of the accuracy estimate (Congalton & Green, 1998). Samples were equally distributed across all classes. Pixel centroids selected for accuracy assessment were greater than 1 m away from training pixels (no overlap). Each sample was evaluated from aerial photography and a class label was assigned. Confusion matrices were constructed from predicted and reference class labels for both islands, and overall and class-specific user's and producer's accuracies were

calculated adjusted for inclusion probabilities associated with the stratified random sample design ((Olofsson et al., 2014) and (Olofsson et al., 2013)). Finally, bias adjusted areas were calculated for each class (Olofsson et al., 2013). All sampling, accuracy assessment and bias adjusted area calculations were coded in R (R Development Core Team & R Core Team, 2024).

2.2.6 Woody Community Class Distribution

We were interested in the distribution of woody plant communities on tree islands and how the proportion of class distributions vary with total tree island woody core area size. For analytical purpose to standardize percent cover calculation of the class distribution of each tree island, we generated two woody core areas that included (1) bayhead shrub, bayhead tree and hammock tree (Woody Core 3), and (2) all woody classes and the mixed woody class (Woody Core 4). For each tree island, woody vegetation classes in the plant community maps were reclassified into a single class, converted from raster to polygon and a 100 m buffer was applied to generate woody core areas. Buffer areas of 100 m were later used to crop the plant community maps and areas were calculated for each class. Class percentages were then calculated for the (1) three woody classes (Woody Core 3), (2) the three woody and herbaceous woody mixed class (Woody Core 4), and (3) for only non-woody classes (Non-Woody). We finally analyzed the relationship between tree island woody core area size (Woody Core 3) and the percentage of woody classes.

2.3 Results and Discussion

2.3.1 Map Accuracy Assessment

Overall accuracy for the four maps ranged from 92.0 ± 1.4 % to 96.5 ± 1.2 % (Table 2.4). Highest accuracies were achieved for the Hammock and Bayhead tree classes ranging from 95.1 ± 2.4 to 100.0 ± 0.0 (Tables 2.5 – 2.8). The inclusion of LiDAR-derived vegetation height metrics has important implications in overall and class-specific accuracies and for the mapping of these communities, hence the high accuracies. The woody class with the lowest accuracy was the mixed woody class with accuracies ranging from 89.2 ± 3.2 to 97.6 ± 1.7. The similarity in spectral signatures of bayhead trees and shrubs explains the low accuracy in this class. All other classes reached accuracies of 91% or greater.

High overall accuracies verify that WV satellite images provide data with characteristics suitable for detecting and mapping tree islands plant communities and their adjacent marshes. Random forest classifiers applied to the bi-seasonal and textural data were able to classify plant communities at high class-specific accuracies. Woody tree and shrub classes were rarely confused with graminoid and broadleaved vegetation in the tails and surrounding marshes. These results indicate that the differentiation between tree islands and their tails and marsh communities is very reliable and that, given the high spatial resolution of the WV data, expansion or contraction of tree islands can be detected as they occur.

Table 2.4 Overall accuracies of classes by image.

Island Name	Bi-Season Data Images (wet/dry)	Overall Accuracy
Vulture, Satinleaf, Gumbo Limbo	2018-02-16/2018-04-17	96.5 ± 1.2 %
NP-202, Irongrape, Black Hammock, Chekika, SS-93, SS-94	2018-02-16/2020-03-28	92.0 ± 1.4 %
SS-81	2018-02-16/2017-05-07	96.5 ± 0.7 %
Grossman Hammock	2018-02-16/2017-05-07	95.0 ± 0.9 %

Table 2.5 Design-based accuracy, area cover in hectares (ha), and adjusted percent cover across Vulture, Satinleaf and Gumbo Limbo (wet/dry WV images: 2018-02-16/2018-04-17).

Class Name	User's Accuracy	Producer's Accuracy
Graminoid Marsh	94.6 ± 2.4	93.2 ± 3.1
Graminoid *Cladium*	95.7 ± 2.1	97.0 ± 1.1
Graminoid *Typha*	91.4 ± 2.9	100.0 ± 0
Herbaceous & Shrub	91.4 ± 2.9	88.0 ± 7.8
Open Marsh	97.8 ± 1.5	97.5 ± 2.3
Bayhead Shrub	100.0 ± 0.0	100.0 ± 0.0
Bayhead Tree	100.0 ± 0.0	100.0 ± 0.0
Hammock Tree	100.0 ± 0.0	100.0 ± 0.0

Table 2.6 Design-based accuracy, area cover in hectares (ha), and adjusted percent cover across Black Hammock, Irongrape, NP-202, Vulture, Chekika, SS-93, and SS-94 (wet/dry WV images: 2018-02-16/2020-03-28).

Class Name	User's Accuracy	Producer's Accuracy
Graminoid Marsh	88.2 ± 3.4	96.0 ± 1.2
Graminoid *Cladium*	94.6 ± 2.4	93.3 ± 1.4
Graminoid *Typha*	84.9 ± 3.7	76.2 ± 15.8
Herbaceous & Shrub	89.2 ± 3.2	71.6 ± 7.7
Open Marsh	90.3 ± 3.1	99.7 ± 0.3
Bayhead Shrub	90.3 ± 3.1	98.9 ± 0.6
Bayhead Tree	97.8 ± 1.5	93.2 ± 4.4
Hammock Tree	100.0 ± 0.0	100.0 ± 0.0

Table 2.7 Design-based accuracy, area cover in hectares (ha), and adjusted percent cover across Heartleaf (SS-81) (wet/dry WV images: 2018-02-16/2017-05-7).

Class Name	User's Accuracy	Producer's Accuracy
Graminoid Marsh	96.3 ± 2.1	99.4 ± 0.4
Graminoid *Cladium*	100.0 ± 0.0	95.9 ± 1.4
Graminoid *Typha*	96.3 ± 2.1	95.3 ± 4.5
Herbaceous & Shrub	93.9 ± 2.7	91.1 ± 3.6
Open Marsh	86.6 ± 3.8	97.8 ± 2.1
Bayhead Shrub	91.5 ± 3.1	96.4 ± 2.1
Bayhead Tree	95.1 ± 2.4	93.4 ± 6.0
Hammock Tree	97.6 ± 1.7	100.0 ± 0.0
Open Water	96.3 ± 2.1	100.0 ± 0.0

Table 2.8 Design-based user's and producer's accuracy for Grossman Hammock (wet/dry WV images: 2018-02-16/2017-05-07).

Class Name	User's Accuracy	Producer's Accuracy
Graminoid Marsh	94.0 ± 2.6	93.7 ± 3.4
Graminoid Marsh Tall	81.0 ± 4.3	76.9 ± 9.5
Graminoid Prairie	98.8 ± 1.2	97.2 ± 1.1
Graminoid Prairie *Cladium*	89.3 ± 3.4	96.5 ± 2.7
Herbaceous & Shrub	97.6 ± 1.7	73.3 ± 7.4
Bayhead Shrub	91.7 ± 3	96.7 ± 1.5
Bayhead Tree	96.4 ± 2	94.2 ± 3.9
Hammock Tree	97.6 ± 1.7	96.7 ± 2.4
Open Water	100.0 ± 0.0	92.1 ± 7.3

2.3.2 Class Distribution by Island

The class distribution of woody area across the eleven islands ranged from 1.45 ha (Satinleaf Island) to 26.06 ha (Grossman Island). Hardwood hammocks occupied a small area in the heads of the eleven mapped islands, ranging from 0.08 ha in SS93 and SS94, located in the Northeast Shark River Slough, to 3.7 ha in Grossman Island, located in the marl prairie. This was expected as compared to tree islands located in the Ridge and Slough, tree islands in the marl prairie are found in higher elevations and are mostly hardwood hammocks which are rarely flooded. The other woody vegetation classes, tree and shrub bayhead, were most abundant in Grossman Island (7.06 ha and 15.3, respectively). The mixed woody vegetation class was higher (14.07 ha) in Heartleaf Island. When changing the size of the core area used to determine vegetation composition, the shrub bayhead class was dominant in all tree islands except for Heartleaf and NP-202 islands where the mixed woody class was dominant (Fig. 2.13).

Graminoid *Cladium* was the most abundant class in ten tree islands (3.56 – 13.99 ha) except for Black Hammock Island, where graminoid marsh was more abundant. The graminoid *Typha* class was higher in Chekika (1.31 ha) and NP-202 (1.23 ha) islands. Chekika is located immediately downstream from the 2.7-mile bridge on Tamiami Trail and is likely to exhibit the impacts of increased high nutrient flow from the WCAs, which might explain the higher composition in *Typha*.

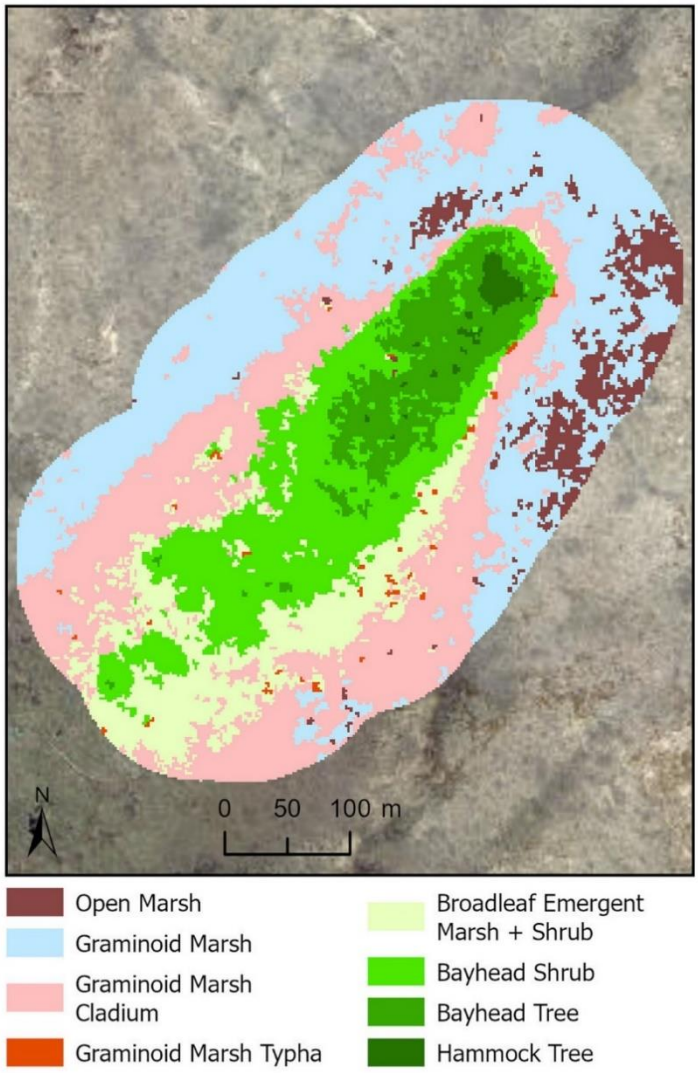

Figure 2.2 Plant communities on Black Hammock Island and the surrounding marsh.

Table 2.9 Class distribution on Black Hammock Island. Area in hectares (ha), and percent for the entire 100 m buffered three-class woody core area. Woody Core 3 (%) = class percentages considering only the three woody classes, Woody Core 4 (%) = class percentage considering the three woody and herbaceous woody mixed class; Non-Woody (%) = class percentages considering only non-woody classes.

Black Hammock Classes	Area (ha)	Percent	Woody Core 3 (%)	Woody Core 4 (%)	Non-Woody (%)
Open Marsh	0.98	5.4	-	-	8.4
Graminoid Marsh	5.67	31.1	-	-	48.9
Cladium	4.88	26.8	-	-	42.1
Typha	0.07	0.4	-	-	0.6
Herbaceous - Shrub Mix	2.23	12.2	-	33.6	-
Bayhead Shrub	2.91	16	66.1	43.9	-
Bayhead Tree	1.36	7.5	30.8	20.5	-
Hardwood Hammock Tree	0.13	0.7	3.1	2	-

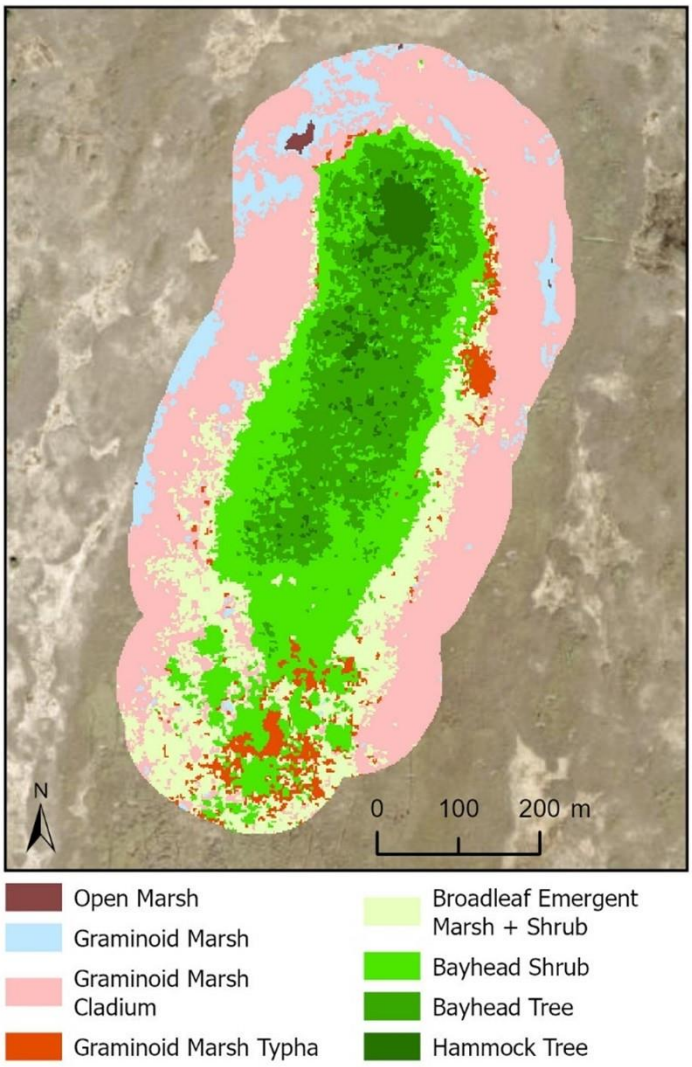

Figure 2.3 Plant communities on Chekika Island and the surrounding marsh.

Table 2.10 Class distribution on Chekika Island. Area in hectares (ha), and percent for the entire 100 m buffered three-class woody core area. Woody Core 3 (%) = class percentages considering only the three woody classes, Woody Core 4 (%) = class percentage considering the three woody and herbaceous woody mixed class; Non-Woody (%) = class percentages considering only non-woody classes.

Chekika Classes	Area (ha)	Percent	Woody Core 3 (%)	Woody Core 4 (%)	Non-Woody (%)
Open Marsh	0.08	0.2	-	-	0.4
Graminoid Marsh	2.01	5.3	-	-	11.5
Cladium	13.99	37.3	-	-	80.5
Typha	1.31	3.5	-	-	7.5
Herbaceous - Shrub Mix	5.61	15	-	27.9	-
Bayhead Shrub	7.8	20.8	53.7	38.8	-
Bayhead Tree	5.71	15.2	39.3	28.4	-
Hardwood Hammock Tree	1.01	2.7	7	5	-

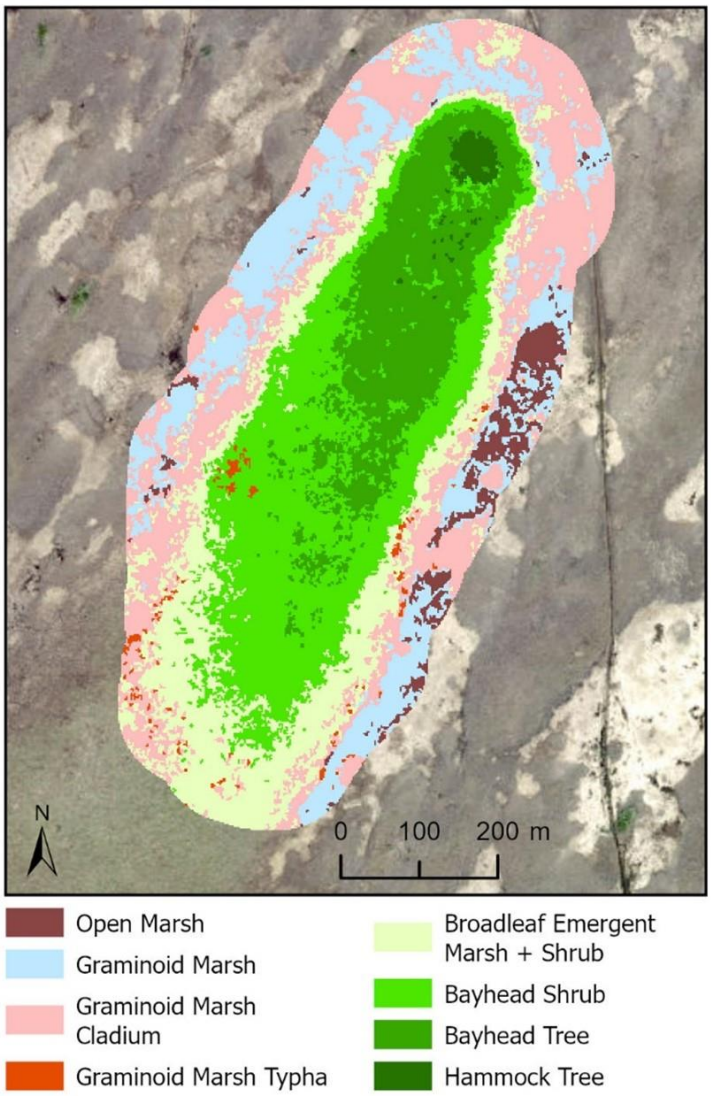

Figure 2.4 Plant communities on Gumbo Limbo Island and the surrounding marsh.

Table 2.11 Class distribution on Gumbo Limbo Island. Area in hectares (ha), and percent for the entire 100 m buffered three-class woody core area. Woody Core 3 (%) = class percentages considering only the three woody classes, Woody Core 4 (%) = class percentage considering the three woody and herbaceous woody mixed class; Non-Woody (%) = class percentages considering only non-woody classes.

Gumbo Limbo Classes	Area (ha)	Percent	Woody Core 3 (%)	Woody Core 4 (%)	Non-Woody (%)
Open Marsh	1.39	3.4	-	-	8.2
Graminoid Marsh	6	14.8	-	-	35.4
Cladium	9.25	22.8	-	-	54.6
Typha	0.3	0.7	-	-	1.8
Herbaceous - Shrub Mix	7.75	19.1	-	32.8	-
Bayhead Shrub	9.51	23.5	59.9	40.3	-
Bayhead Tree	6	14.8	37.8	25.4	-
Hardwood Hammock Tree	0.37	0.9	2.3	1.6	-

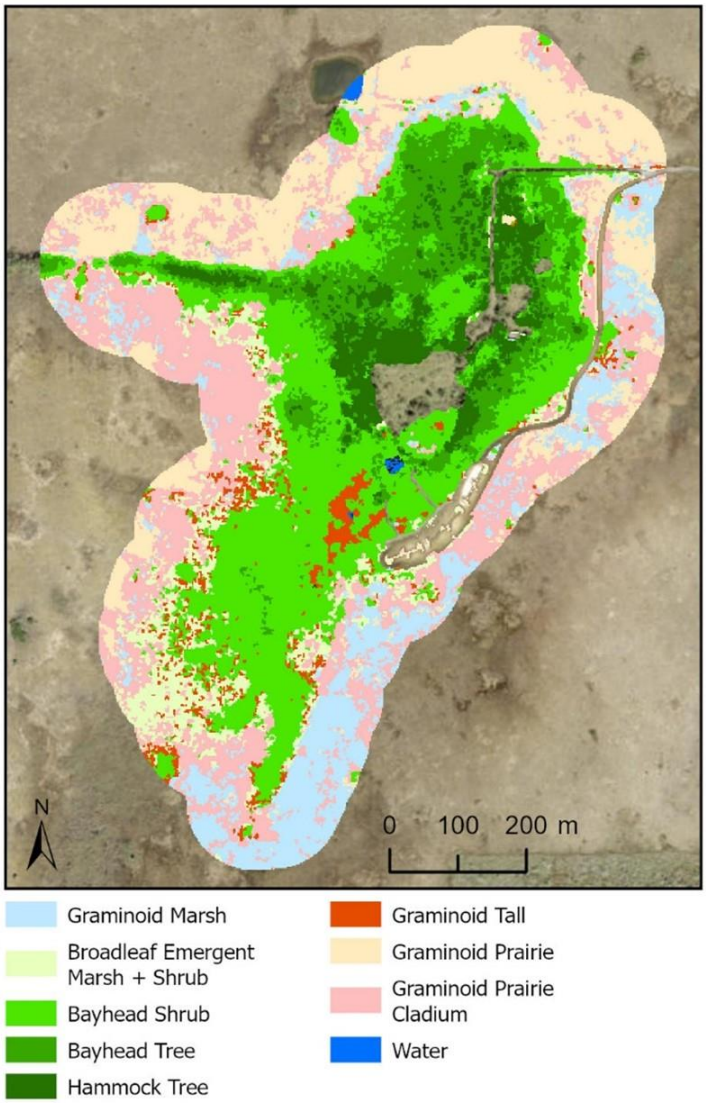

Figure 2.5 Plant communities on Grossman Island and the surrounding marsh.

Table 2.12 Class distribution on Grossman Island. Area in hectares (ha), and percent for the entire 100 m buffered three-class woody core area. Woody Core 3 (%) = class percentages considering only the three woody classes, Woody Core 4 (%) = class percentage considering the three woody and herbaceous woody mixed class; Non-Woody (%) = class percentages considering only non-woody classes.

Grossman Classes	Area (ha)	Percent	Woody Core 3 (%)	Woody Core 4 (%)	Non-Woody (%)
Graminoid Marsh	6.68	10.7	-	-	20.8
Graminoid Marsh Tall	2.01	3.2	-	-	6.3
Herbaceous - Shrub Mix	4.14	6.6	-	13.7	-
Graminoid Prairie	9.89	15.9	-	-	30.8
Graminoid Prairie *Cladium*	13.37	21.5	-	-	41.7
Bayhead Shrub	15.3	24.6	58.7	50.7	-
Bayhead Tree	7.06	11.3	27.1	23.4	-
Hardwood Hammock Tree	3.7	5.9	14.2	12.2	-
Open Water	0.1	0.2	-	-	0.3

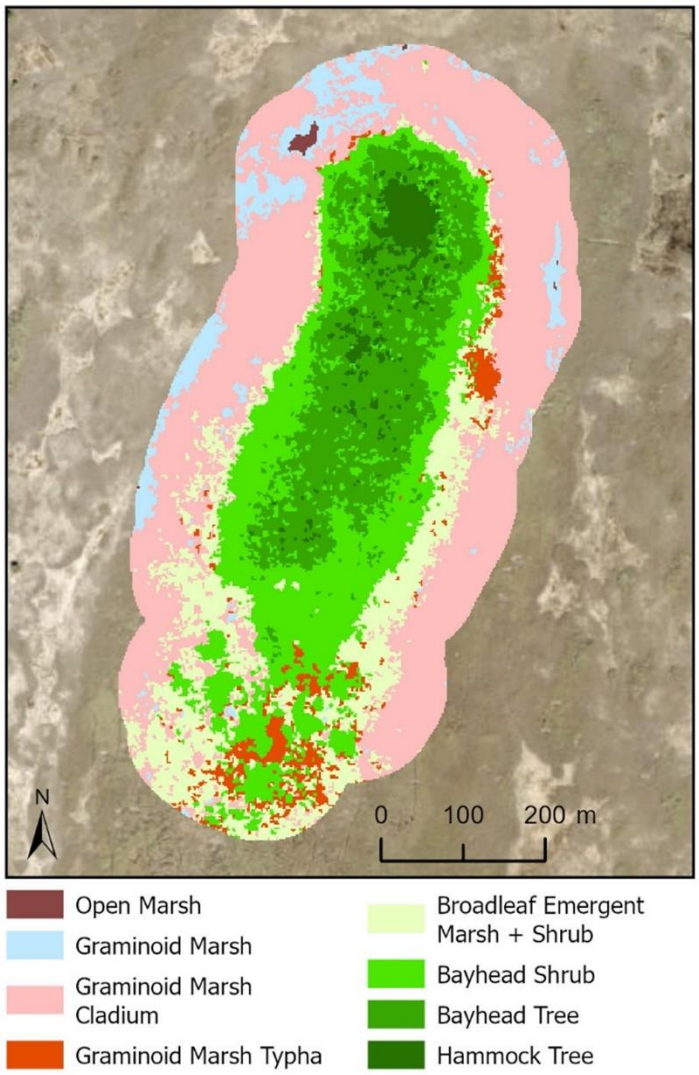

Figure 2.6 Plant communities on Heartleaf Island and the surrounding marsh.

Table 2.13 Class distribution on Heartleaf Island. Area in hectares (ha), and percent for the entire 100 m buffered three-class woody core area. Woody Core 3 (%) = class percentages considering only the three woody classes, Woody Core 4 (%) = class percentage considering the three woody and herbaceous woody mixed class; Non-Woody (%) = class percentages considering only non-woody classes.

Heartleaf Classes	Area (ha)	Percent	Woody Core 3 (%)	Woody Core 4 (%)	Non-Woody (%)
Open Marsh	0.81	2.1	-	-	10.1
Graminoid Marsh	0.6	1.5	-	-	7.4
Cladium	5.66	14.6	-	-	70.5
Typha	0.96	2.5	-	-	11.9
Herbaceous - Shrub Mix	14.07	36.4	-	45.9	-
Bayhead Shrub	12.12	31.3	73.1	39.5	-
Bayhead Tree	3.88	10	23.4	12.7	-
Hardwood Hammock Tree	0.58	1.5	3.5	1.9	-

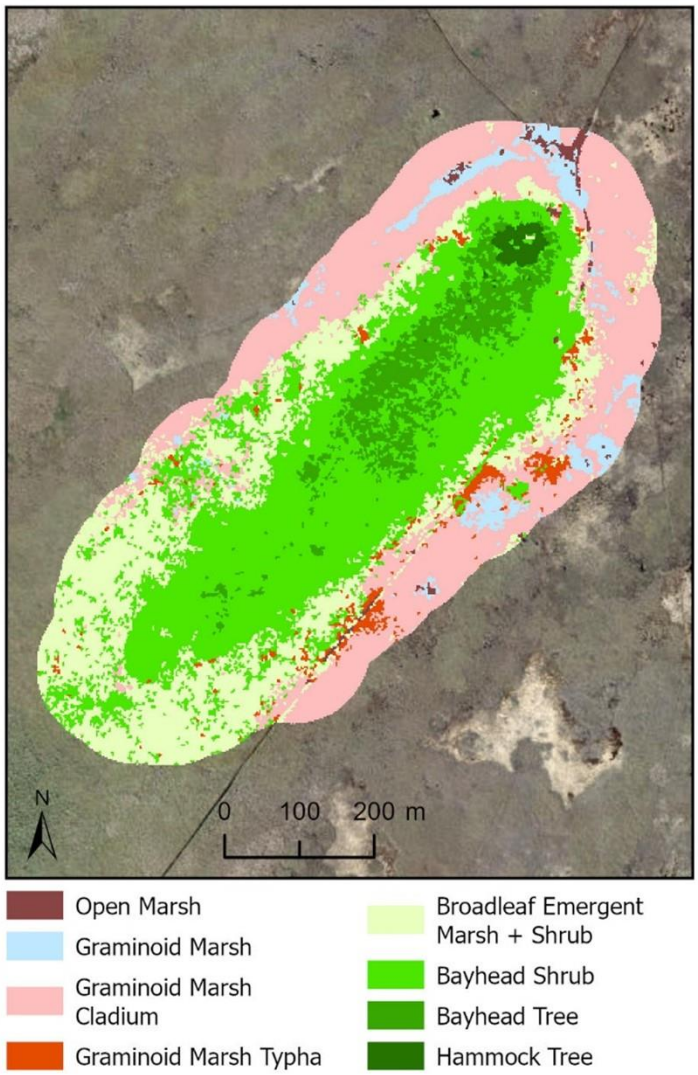

Figure 2.7 Plant communities on Irongrape Island and the surrounding marsh.

Table 2.14 Class distribution on Irongrape Island. Area in hectares (ha), and percent for the entire 100 m buffered three-class woody core area. Woody Core 3 (%) = class percentages considering only the three woody classes, Woody Core 4 (%) = class percentage considering the three woody and herbaceous woody mixed class; Non-Woody (%) = class percentages considering only non-woody classes.

Irongrape Classes	Area (ha)	Percent	Woody Core 3 (%)	Woody Core 4 (%)	Non-Woody (%)
Open Marsh	0.3	0.8	-	-	2.3
Graminoid Marsh	1.45	3.6	-	-	10.7
Cladium	10.87	26.8	-	-	80.5
Typha	0.89	2.2	-	-	6.6
Herbaceous - Shrub Mix	9.62	23.7	-	35.5	-
Bayhead Shrub	14.34	35.3	82.2	53	-
Bayhead Tree	2.8	6.9	16	10.3	-
Hardwood Hammock Tree	0.31	0.8	1.8	1.2	-

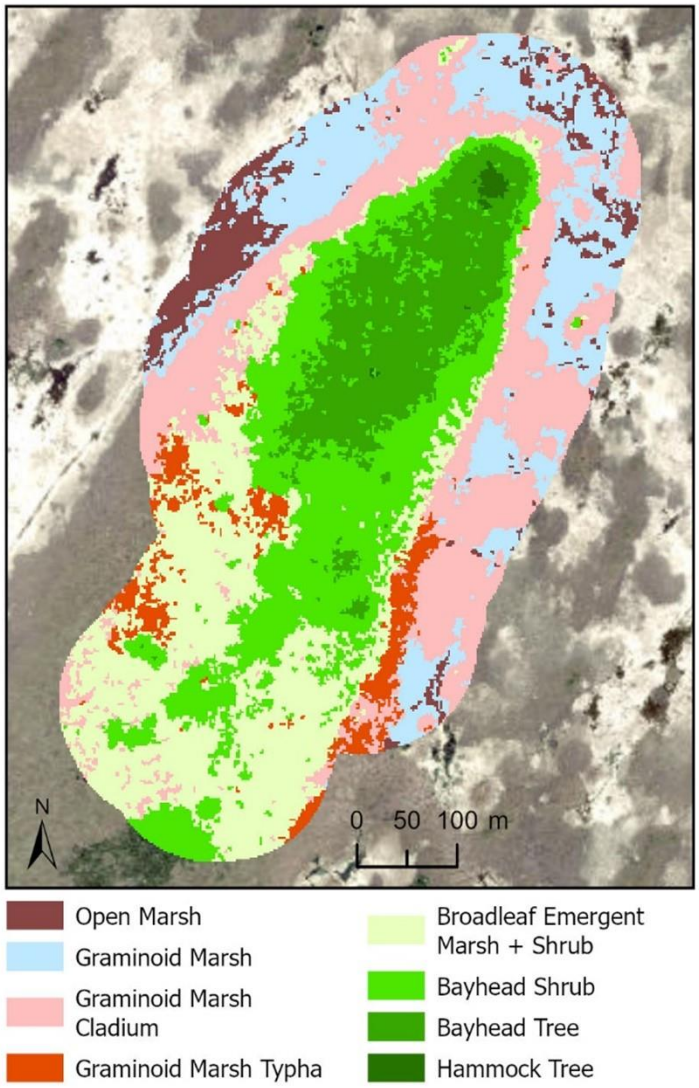

Figure 2.8 Tree Island plant communities on NP-202 Island and the surrounding marsh.

Table 2.15 Class distribution on NP-202 Island. Area in hectares (ha), and percent for the entire 100 m buffered three-class woody core area. Woody Core 3 (%) = class percentages considering only the three woody classes, Woody Core 4 (%) = class percentage considering the three woody and herbaceous woody mixed class; Non-Woody (%) = class percentages considering only non-woody classes.

NP-202 Classes	Area (ha)	Percent	Woody Core 3 (%)	Woody Core 4 (%)	Non-Woody (%)
Open Marsh	1.41	4.8	-	-	10.7
Graminoid Marsh	4.25	14.5	-	-	32.1
Cladium	6.35	21.7	-	-	48
Typha	1.23	4.2	-	-	9.3
Herbaceous - Shrub Mix	6.65	22.7	-	41.3	-
Bayhead Shrub	5.85	19.9	61.9	36.3	-
Bayhead Tree	3.52	12	37.2	21.8	-
Hardwood Hammock Tree	0.09	0.3	0.9	0.5	-

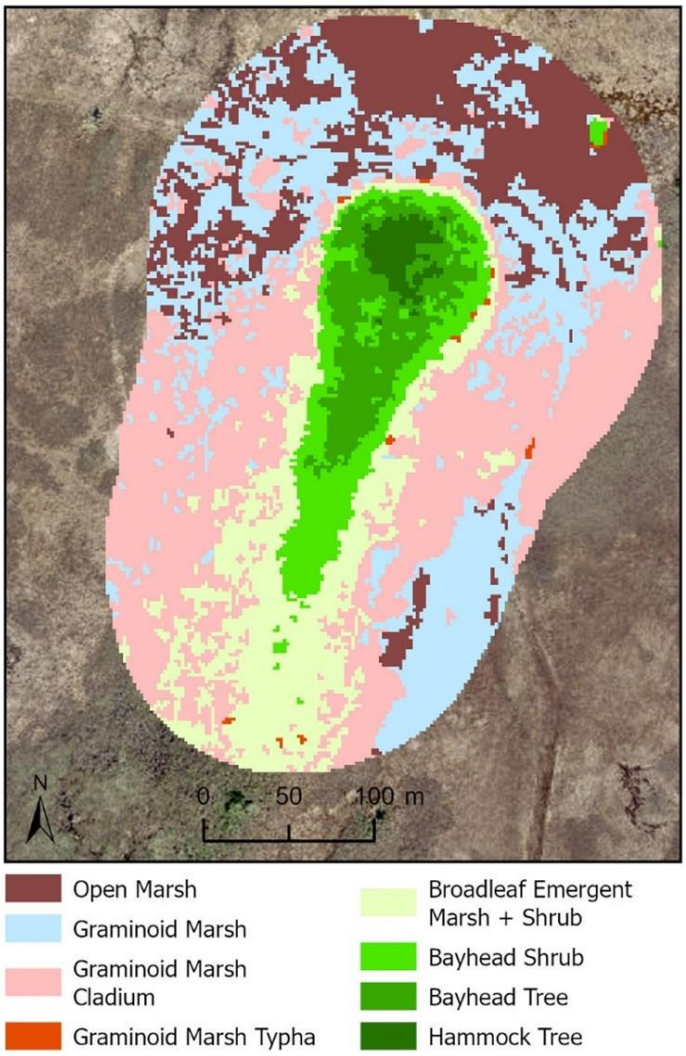

Figure 2.9 Plant communities on Satinleaf Island and the surrounding marsh.

Table 2.16 Class distribution on Satinleaf Island. Area in hectares (ha), and percent for the entire 100 m buffered three-class woody core area. Woody Core 3 (%) = class percentages considering only the three woody classes, Woody Core 4 (%) = class percentage considering the three woody and herbaceous woody mixed class; Non-Woody (%) = class percentages considering only non-woody classes.

Satinleaf Classes	Area (ha)	Percent	Woody Core 3 (%)	Woody Core 4 (%)	Non-Woody (%)
Open Marsh	1.91	17.7	-	-	24.4
Graminoid Marsh	2.35	21.7	-	-	29.9
Cladium	3.56	32.9	-	-	45.4
Typha	0.02	0.2	-	-	0.3
Herbaceous - Shrub Mix	1.53	14.1	-	51.4	-
Bayhead Shrub	0.7	6.4	48.2	23.4	-
Bayhead Tree	0.6	5.6	41.6	20.2	-
Hardwood Hammock Tree	0.15	1.4	10.1	4.9	-

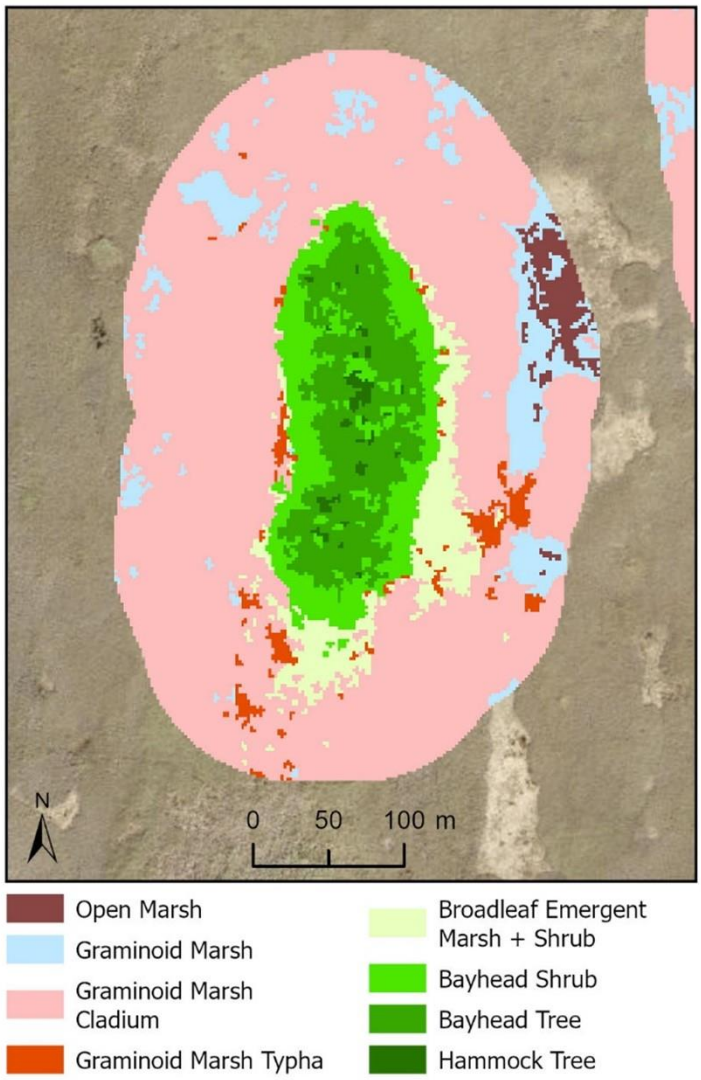

Figure 2.10 Plant communities on SS93 Island and the surrounding marsh.

Table 2.17 Class distribution on SS93 Island. Area in hectares (ha), and percent for the entire 100 m buffered three-class woody core area. Woody Core 3 (%) = class percentages considering only the three woody classes, Woody Core 4 (%) = class percentage considering the three woody and herbaceous woody mixed class; Non-Woody (%) = class percentages considering only non-woody classes.

SS93 Classes	Area (ha)	Percent	Woody Core 3 (%)	Woody Core 4 (%)	Non-Woody (%)
Open Marsh	0.25	2	-	-	2.6
Graminoid Marsh	0.93	7.4	-	-	9.8
Cladium	8	63.7	-	-	84.7
Typha	0.27	2.2	-	-	2.9
Herbaceous - Shrub Mix	0.75	6	-	24.3	-
Bayhead Shrub	1.12	8.9	47.6	36	-
Bayhead Tree	1.15	9.2	49.1	37.2	-
Hardwood Hammock Tree	0.08	0.6	3.3	2.5	-

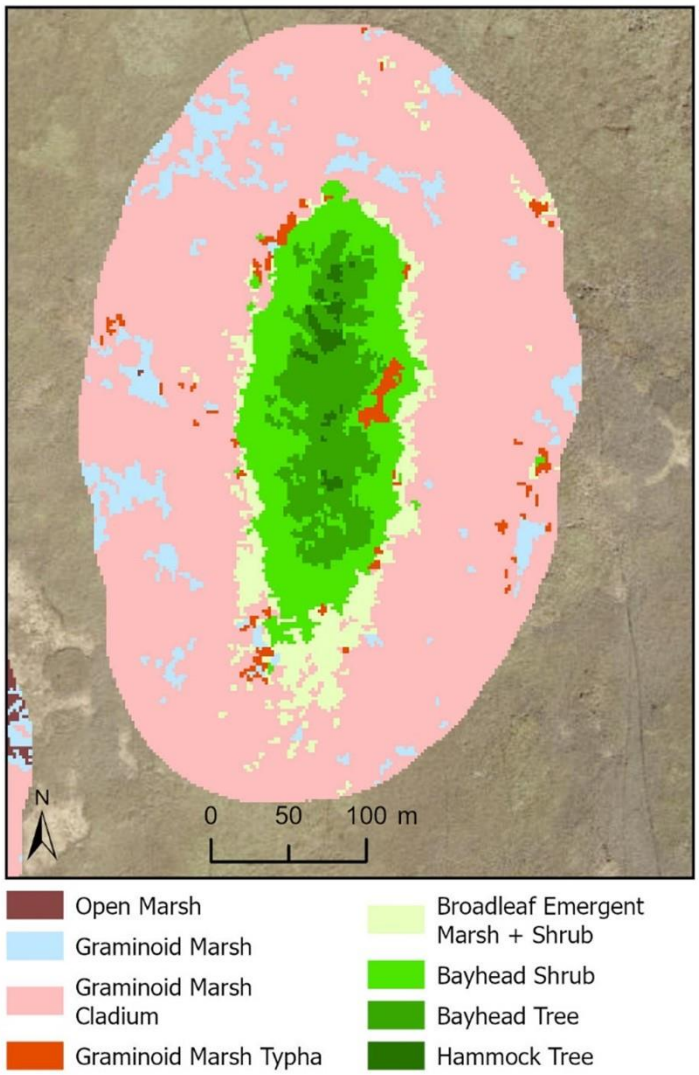

Figure 2.11 Plant communities on SS94 Island and the surrounding marsh.

Table 2.18 Class distribution on SS94 Island. Area in hectares (ha), and percent for the entire 100 m buffered three-class woody core area. Woody Core 3 (%) = class percentages considering only the three woody classes, Woody Core 4 (%) = class percentage considering the three woody and herbaceous woody mixed class; Non-Woody (%) = class percentages considering only non-woody classes.

SS94 Classes	Area (ha)	Percent	Woody Core 3 (%)	Woody Core 4 (%)	Non-Woody (%)
Open Marsh	0	0	-	-	0
Graminoid Marsh	0.74	5.8	-	-	7.6
Cladium	8.8	69.3	-	-	90.5
Typha	0.18	1.4	-	-	1.8
Herbaceous - Shrub Mix	0.75	5.9	-	25	-
Bayhead Shrub	1.34	10.6	60.1	45	-
Bayhead Tree	0.81	6.4	36.2	27.2	-
Hardwood Hammock Tree	0.08	0.6	3.7	2.8	-

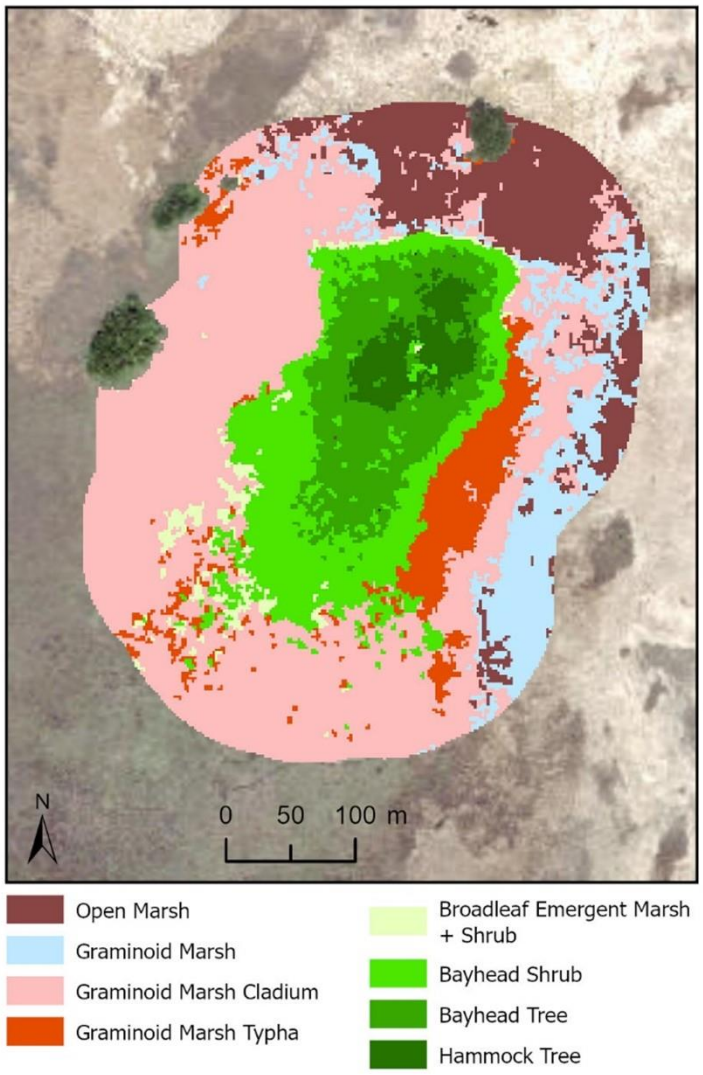

Figure 2.12 Plant communities on Vulture Island and the surrounding marsh.

Table 2.19 Class distribution on Vulture Island. Area in hectares (ha), and percent for the entire 100 m buffered three-class woody core area. Woody Core 3 (%) = class percentages considering only the three woody classes, Woody Core 4 (%) = class percentage considering the three woody and herbaceous woody mixed class; Non-Woody (%) = class percentages considering only non-woody classes.

Vulture Classes	Area (ha)	Percent	Woody Core 3 (%)	Woody Core 4 (%)	Non-Woody (%)
Open Marsh	2.11	12.2	-	-	17.3
Graminoid Marsh	1.6	9.3	-	-	13.1
Cladium	7.32	42.4	-	-	60
Typha	1.17	6.8	-	-	9.6
Herbaceous - Shrub Mix	0.35	2	-	6.9	-
Bayhead Shrub	2.47	14.3	52.5	48.9	-
Bayhead Tree	1.71	9.9	36.2	33.7	-
Hardwood Hammock Tree	0.54	3.1	11.4	10.6	-

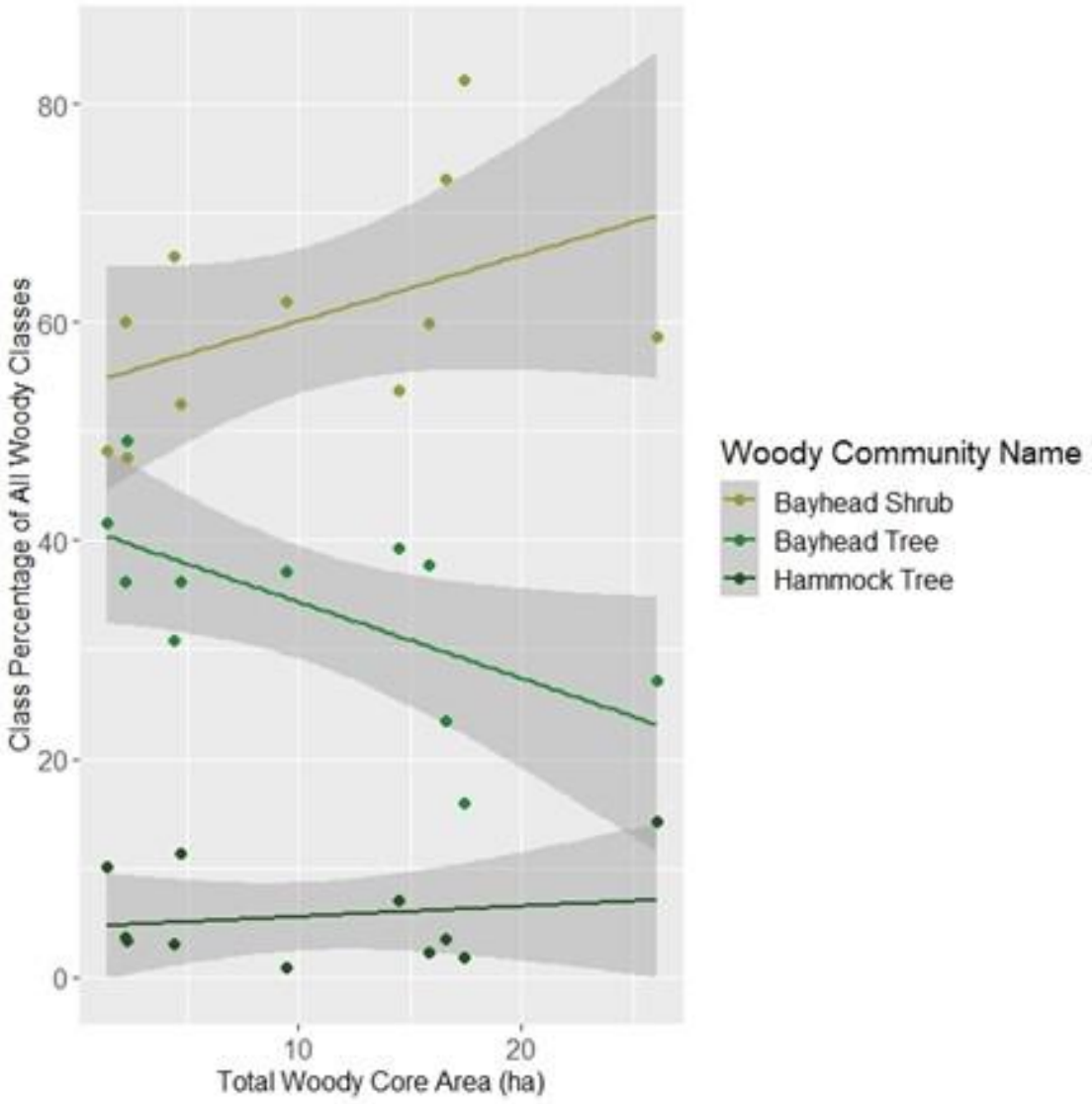

Figure 2.13 Class percentage of the three woody core classes as a function of total core area.

Acknowledgments

We would like to acknowledge the assistance in the field (2021-2022) by our lab members Carlos Pulido, Jessica Rios, Katherine Castrillon, Christian Prieto, and Myranda Hernandez. We also would like to thank our lab member Erica Garcia who help in data processing. We are also thankful to Pablo Ruiz (ENP) for his active role during the early 2000s in establishing a network of tree islands for monitoring within Everglades National Park. The project received financial support from the RECOVER working group within the Comprehensive Everglades Restoration Plan (CERP). The support from the RECOVER working group was provided through the U.S. Army Corps of Engineers (U.S. Army Engineer Research & Development Center) with Cooperative Agreement Number W912HZ-19-2-0032. This study was allowed under Permit EVER-2022-SCI-0011.

Literature Cited

Abtew, W. and Ciuca, V. (2017). *South Florida Hydrology and Water Management. In: 2017 South Florida Environmental Report Volume 1*. South Florida Water Management District (SFWMD).

Armentano, T. V., Jones, D. T., Ross, M. S. and Gamble, B. W. (2002). Vegetation pattern and process in tree islands of the southern Everglades and adjacent areas. In F. H. Sklar & A. van der Valk (Eds.), *Tree Islands of the Everglades* (pp. 225–282). Kluwer Academic Publishers.

Armentano, T. V., Sah, J. P., Ross, M. S., Jones, D. T., Cooley, H. C. and Smith, C. S. (2006). Rapid responses of vegetation to hydrological changes in Taylor Slough, Everglades National Park, Florida, USA. *Hydrobiologia* **569** (1): 293–309.

Barnes, E. M., Clarke, T. R., Richards, S. E., Colaizzi, P. D., Haberland, J., Kostrzewski, M., Waller, P., Choi, C., Riley, E., Thompson, T. and Others. (2000). Coincident detection of crop water stress, nitrogen status and canopy density using ground based multispectral data. *Proceedings of the Fifth International Conference on Precision Agriculture, Bloomington, MN, USA, 1619*. https://naldc.nal.usda.gov/download/4190/PDF

Bernhardt, C. E. and Willard, D. A. (2009). Response of the Everglades ridge and slough landscape to climate variability and 20th-century water management. *Ecological Applications: A Publication of the Ecological Society of America* **19** (7): 1723–1738.

Brandt, L. A., Portier, K. M. and Kitchens, W. M. (2000). Patterns of change in tree islands in Arthur R. Marshall Loxahatchee National Wildlife Refuge from 1950 to 1991. *Wetlands* **20** (1): 1–14.

Breiman, L. (2001). Random Forests. *Machine Learning* **45** (1), 5–32.

Cangialosi, J. P., Latto, A. S. and Berg, R. (2018). National Hurricane Center tropical cyclone report: Hurricane Irma. *National Oceanic and Atmospheric Administration: May 30*.

Congalton, R. G., and Green, K. (1999). Assessing the accuracy of remotely sensed data: principles and practices. Page 137. Lewis Publishers, Boca Raton, Florida 33431.

Cortez, N. A. (2024). *Chapter 2A: South Florida Hydrology and Water Management*. In: 2024 South Florida Environmental Report, Vol. 1, pp. 2A-1 to 2A-59. South Florida Water Management District, West Palm Beach, FL

Cortez, N. A., Qiu, C. and Ciuca, V. (2022). *Chapter 2*: *South Florida Hydrology and Water Management*. In: 2022 The South Florida Environmental Report, Vol. 1, pp. 2A-1 to 2A-46. South Florida Water Management District, West Palm Beach, FL.

Daughtry, C. S. T., Walthall, C. L., Kim, M. S., de Colstoun, E. B. and McMurtrey, J. E. (2000). Estimating Corn Leaf Chlorophyll Concentration from Leaf and Canopy Reflectance. *Remote Sensing of Environment* **74** (2): 229–239.

Delegido, J., Verrelst, J., Alonso, L. and Moreno, J. (2011). Evaluation of Sentinel-2 red-edge bands for empirical estimation of green LAI and chlorophyll content. *Sensors* **11** (7): 7063–7081.

Donnelly, M. J. and Walters, L. J. (2008). Water and boating activity as dispersal vectors for *Schinus terebinthifolius* (Brazilian pepper) seeds in freshwater and estuarine habitats. *Estuaries and Coasts* **31** (5): 960-968.

Espinar, J. L., Ross, M. S. and Sah, J. P. (2011). Pattern of nutrient availability and plant community assemblage in Everglades tree islands, Florida, USA. *Hydrobiologia* **667**: 89–99.

Ewel, J. J., Ojima, D. S., Karl, D. A. and DeBusk, W. F. (1982). *Schinus* in successional ecosystems of Everglades National Park. Report T-676. U.S. Everglades National Park, South Florida Research Center, Homestead, FL. 141 pp.

Exelis Visual Information Solutions. (2013). CMedia B. V., Emmeloord, Netherlands, Emmeloord.

Frazer, G. W., Canham, C. D. and Lertzman, K. P. (1999). Imaging software to extract canopy structure and gap light transmission indices from true-colour fisheye photographs, users' manual, and program documentation. *Millbrook, New York*.

Gann, D. 2018. *Quantitative Spatial Upscaling of Categorical Data in the Context of Landscape Ecology: A New Scaling Algorithm*. PhD. Biology, Florida International University.

Gann, D. and Richards, J. (2023). Scaling of classification systems—effects of class precision on detection accuracy from medium resolution multispectral data. *Landscape Ecology*, **38** (3): 659–687.

Gitelson, A. A., Kaufman, Y. J. and Merzlyak, M. N. (1996). Use of a green channel in remote sensing of global vegetation from EOS-MODIS. *Remote Sensing of Environment* **58** (3): 289–298.

Givnish, T., Volin, J., Owen, D., Volin, V., Muss, J. and Glaser, P. (2008). Vegetation differentiation in the patterned landscape of the central Everglades: Importance of local and landscape drivers. *Global Ecology and Biogeography: A Journal of Macroecology* **17:** 384–402.

Hanan, E. J. and Ross, M. S. (2010). Across-scale patterning of plant-soil-water interactions surrounding tree islands in southern Everglades landscapes. *Landscape Ecology* **25** (3): 463–475.

Hochmair, H. H., Benjamin, A., Gann, D., Juhász, L., Olivas, P., & Fu, Z. J. (2022). Change Analysis of Urban Tree Canopy in Miami-Dade County. *Forests, Trees and Livelihoods*, **13** (6): 949.

Hook, D. D. (1984). Waterlogging tolerance of lowland tree species of the South. *Southern Journal of Applied Forestry*. **8** (3): 136-149.

Huete, A. (1988). A soil-adjusted vegetation index (SAVI). Remote Sensing of Environment. *Remote Sensing of Environment* **25**: 295–309.

Jiang, Z., Huete, A. R., Didan, K. and Miura, T. (2008). Development of a two-band enhanced vegetation index without a blue band. *Remote Sensing of Environment* **112** (10): 3833–3845.

Kennedy, H. (1990). *Celtis laevigata* Willd., Sugarberry. In: Burns, R.M.; Honkala, B.H., tech. cords. Silvics of North America: Vol. 2. Hardwoods. Agriculture Handbook 654. Washington, DC: U.S. Department of Agriculture: 258-261.

Kuhn, M., Wing, J., Weston, S., Williams, A., Keefer, C., Engelhardt, A., Cooper, T., Mayer, Z., Kenkel, B., Team, T. R. C., Benesty, M., Lescarbeau, R., Ziem, A. and Scrucca, L. (2015). *caret: Classification and Regression Training*.

Kuhn, M. (2019). "The Caret Package: Classification and Regression Training." Comput Vienna, Austria.

Lemmon, P. E. (1956). *A spherical densitometer for estimating forest overstory density* Vol. 2: 314–320.

McFeeters, S. K. (1996). The use of the Normalized Difference Water Index (NDWI) in the delineation of open water features. *International Journal of Remote Sensing* **17** (7): 1425–1432.

Nocentini, A., Redwine, J., Gaiser, E., Hill, T., Hoffman, S., Kominoski, J., Sah, J., Shinde, D., Surratt, D. (2024). Rehydration of degraded wetlands: understanding drivers of vegetation community trajectories. *Ecosphere* 2024; 15: e4813. doi: 10.1002/ecs2.4813.

Oksanen, J., Simpson, G,. Blanchet, F., et al., (2022). _vegan: Community Ecology Package_. R package version 2.6-2, <https://CRAN.R-project.org/package=vegan>.

Olofsson, P., Foody, G. M., Herold, M., Stehman, S. V., Woodcock, C. E. and Wulder, M. A. (2014). Good practices for estimating area and assessing accuracy of land change. *Remote Sensing of Environment* **148**: 42–57.

Olofsson, P., Foody, G. M., Stehman, S. V. and Woodcock, C. E. (2013). Making better use of accuracy data in land change studies: Estimating accuracy and area and quantifying uncertainty using stratified estimation. *Remote Sensing of Environment* **129**:122–131.

Parker, G. G. (1995). Structure and microclimate of forest canopies. In M. Lowman & N. Nadkarni (Eds.), *Forest canopies: a review of research on a biological frontier*. Academic Press.

Patterson, K., & Finck, R. (1999). *Tree islands of WCA3: Aerial photointerpretation and trend analysis project summary report*.

R Core Team. (2024). *R: A Language and Environment for Statistical Computing*. R Foundation for Statistical Computing. https://www.R-project.org/

RECOVER. (2009). *Revised CERP Monitoring and Assessment Plan. Restoration Coordination and Verification Program c/o US Army Corps of Engineers, Jacksonville District, Jacksonville, FL, and South Florida Water Management District, West Palm Beach, FL*.

RECOVER. (2011). *RECOVER: Performance Measures Greater Everglades*. http://141.232.10.32/pm/recover/perf_ge.aspx

RECOVER. (2020). *The Recover Team's Recommendations for Interim Goals and Interim Targets for the Comprehensive Everglades Restoration Plan*. https://pdfs.semanticscholar.org/b545/b09e4581c654f936945ea769f9a285465c5b.pdf

Ross, M. S. and Jones, D. T. (2004). *Tree islands in the Shark Slough landscape: interactions of vegetation, hydrology and soils. Final Report to Everglades National Park, EVER 00075*. https://digitalcommons.fiu.edu/sercrp/4/

Ross, M. S. and Sah, J. P. (2011). Forest Resource Islands in a Sub-tropical Marsh: Soil–Site Relationships in Everglades Hardwood Hammocks. *Ecosystems* **14**, 632–645.

Ross, M. S., Mitchell-Bruker, S., Sah, J. P., Stothoff, S., Ruiz, P. L., Reed, D. L., Jayachandran, K. and Coultas, C. L. (2006). Interaction of hydrology and nutrient limitation in the Ridge and Slough landscape of the southern Everglades. *Hydrobiologia* **569**, 37–59.

Ross, M. S., Stoffella, S., Vidales, R., Meeder, J. F., Kadko, D. C., Scinto, L. J., Subedi, S. C. and Redwine, J. (2022). Sea-Level Rise and the persistence of tree islands in coastal landscapes. *Ecosystems* **25**: 586–602.

Rouse, J. W., Haas, R. H., Schell, J. A. and Deering, D. W. (1974). Monitoring Vegetation Systems in the Great Plains with ERTS Proceeding. *Third Earth Reserves Technology Satellite Symposium, Greenbelt: NASA SP-351, 30103017*.

Ruiz, P. L., Ross, M. S. and Sah, J. P. (2013). Monitoring of Tree Island Condition in the Southern Everglades: Hydrologic Driven Decadal Changes in Tree Island Woody Vegetation Structure and Composition. US Army Engineer Research and Development Center. 41 pp.

Ruiz, P. L., Sah, J. P., Ross, M. S., Rodriguez, D. and Lambert, A. (2011). Monitoring of Tree Island Conditions in the Southern Everglades: The Effects of Hurricanes and Hydrology on the Status and Population Dynamics of Sixteen Tropical Hardwood Hammock Tree Islands. US Army Engineer Research and Development Center. 136 pp.

Sah, J. P. (2004). *Vegetation Structure and Composition in Relation to the Hydrological and Soil Environments in Tree Islands of Shark Slough*. In M. S. Ross & D. T. Jones (Eds.) Tree Islands in the Shark Slough Landscape: Interactions of Vegetation, Hydrology and Soils. (pp. 85–114). A Final Report Submitted to Everglades National Park, National Park Service, U.S. Department of the Interior, USA.

Sah, J. P., Gann, D., Ross, M.S, Mesa, X., Olivas, P., Stoffella, S. and Constant, B. (2020). Monitoring of Tree Island Condition in the Southern Everglades. Year-5 Report (2014-2019). Submitted to US Army Engineer Research and Development Center. June 2020. 107 pp.

Sah, J. P., Mesa, X., Gann, D., Ross, M.S, Stoffella, S. and Constant, B. (2021). Monitoring of Tree Island Condition in the Southern Everglades. Year-1 Report (2019-2020). Submitted to US Army Engineer Research & Development Center. March 2021. 45 pp.

Sah, J. P., Mesa, X., Gann, D., Ross, M.S, Stoffella, S. and Constant, B. (2022). Monitoring of Tree Island Condition in the Southern Everglades. Year-2 Report (2020-2021). Submitted to US Army Engineer Research & Development Center. June 2022. 49 pp.

Sah, J. P., Mesa, X., Ross, M. S., Gann, D., Stoffella, S., Constant, B. and Castaneda, S. (2023). Monitoring of Tree Island Condition in the Southern Everglades. Year-3 Report (2019-2022). Submitted to US Army Engineer Research & Development Center. November 2023. 47 pp.

Sah, J. P., Ross, M. S., Ruiz, P. L. and Subedi, S. (2012). Monitoring of Tree Island in the Southern Everglades. Annual Report-2011. Cooperative Agreement: W912HZ-09-2-0019. US Army Engineer Research and Development Center. 72 pp.

Sah, J. P., Ross, M. S., Ruiz, P., Freixa, J. and Stoffella, S. (2015). Monitoring or Tree Island Condition in the Southern Everglades. Annual Report submitted to US Army Engineer Research and Development Center. Report (2011-2014). April 2015. 100 pp.

Sah, J. P., Ruiz, P. L. and Ross, M. S. (2018). Spatio-temporal pattern of plant communities along a hydrologic gradient in Everglades tree islands. *Forest Ecology and Management* **421**: 16–31.

Sarker, S. K., J. S. Kominoski, E. E. Gaiser, L. J. Scinto, and D. T. Rudnick. 2020. Quantifying effects of increased hydroperiod on wetland nutrient concentrations during early phases of freshwater restoration of the Florida Everglades. *Restoration Ecology* 28:1561-1573.

Shamblin, B., Ross, M. S., Oberbauer, S. F., Gomez, D., Sternberg, L., Saha, A., & Wang, X. (2008). CERP monitoring and assessment program: tree island conditions in the southern Everglades. Annual Report for 2007 submitted to the South Florida Natural Resources Center, Everglades National Park, Homestead, FL.

Sklar, F. H., Richards, J., Gann, D., Dreschel, T., Larsen, L. G., Newman, S., Coronado-Molina, C., Schall, T., Saunders, C. J., Harvey, J. W. and Santamaria, F. (2013). *Chapter 6: Everglades Research and Evaluation - Landscape* (F. H. Sklar & T. Dreschel (Eds.); The South Florida Environmental Report, Vol. 1, pp. 6–62 to 6–75). South Florida Water Management District.

Stoffella, S. L., Ross, M. S., Sah, J. P., Price, R. M., Sullivan, P. L., Cline, E. A. and Scinto, L. J. (2010). Survival and growth responses of eight Everglades tree species along an experimental hydrological gradient on two tree island types. *Applied Vegetation Science*, **13** (4), 439–449.

Stoffella, S. L., Ross, M. S., Sah, J. P., Price, R. M., Scinto, L. J., Cline, E. A. and Sklar, F> H. (2022). Flooding and planting density shape forests in an experimental Everglades landscape: Lessons for forest restoration. *Ecosphere*, 2022; 13:e4223.

Stone, P. A., & Chmura, G. L. (2004). *Sediments, stratigraphy, and aspects of succession, chronology, and major prehistoric disturbance in the principal type of large tree island in Shark Slough* (Tree Islands in the Shark Slough Landscape: Interactions of Vegetation, Hydrology and Soils. Final Report, pp. 17–29). Ross, M. S.

Sullivan, P. L., Engel, V., Ross, M. S. and Price, R. M. (2013). The influence of vegetation on the hydrodynamics and geomorphology of a tree island in Everglades National Park, (Florida, United States). *Ecohydrology*, DOI: 10.1002/eco.1394.

Sullivan, P. L., Price, R. M., Ross, M. S., Scinto, L. J., Stoffella, S. L., Cline, E., Dreschel, T. W. and Sklar, F. H. (2010). Hydrologic processes on tree islands in the Everglades (Florida, USA): tracking the effects of tree establishment and growth. *Hydrogeology Journal*, *doi: 10.1007/s10040-010-0691-0*.

Tassin, J., Riviere, J. and Clergeau, P. (2007). Reproductive versus vegetative recruitment of the invasive tree *Schinus terebinthifolius*: implications for restoration on Reunion Island. *Restoration Ecology* **15** (3): 412-419.

USACE. (2014). *CERP – Central Everglades Planning Project (CEPP): Final Integrated Project Implementation Report and Environmental Impact Statement*. U.S. Army Corps of Engineers.

USACE. (2020). *Final Environmental Impact Statement - Combine Operation Plan*. U.S. Army Corps of Engineers. Jacksonville District, Jacksonville, FL. 476 pp.

USACE (U.S. Army Corps of Engineers), ENP (Everglades National Park) and SFMWD (South Florida Water Management District) (2023) Combined Operational Plan (COP) Biennial Report-2023.

Wendelberger, K. S., Gann, D. and Richards, J. H. (2018). Using Bi-seasonal worldview-2 multi-spectral data and supervised random forest classification to map coastal plant communities in everglades national park. *Sensors*, ***18*** (3): doi.org/10.3390/s18030829

Wetzel, P. R. (2002). Analysis of Tree Island Vegetation Communities. In F. H. Sklar & A. Van Der Valk (Eds.), *Tree Islands of the Everglades* (pp. 357–389). Springer Netherlands.

Wetzel, P. R., Pinion, T., Towles, D. T. and Heisler, L. (2008). Landscape analysis of tree island head vegetation in water conservation Area 3, Florida Everglades. *Wetlands* **28:** 276–289.

Wetzel, P. R., Sah, J. P. and Ross, M. S. (2017). Tree islands: the bellwether of Everglades ecosystem function and restoration success. *Restoration Ecology* **25** (S1): S71–S85.

Wetzel, P. R., van der Valk, A. G., Newman, S., Gawlik, D. E., Troxler Gann, T., Coronado-Molina, C. A., Childers, D. L. and Sklar, F. H. (2005). Maintaining tree islands in the Florida Everglades: nutrient redistribution is the key. *Frontiers in Ecology and the Environment* **3** (7), 370–376.

Zweig, C. L. and Kitchens, W. M. (2009). Multi-state succession in wetlands: a novel use of state and transition models. *Ecology* **90** (7): 1900–1909.